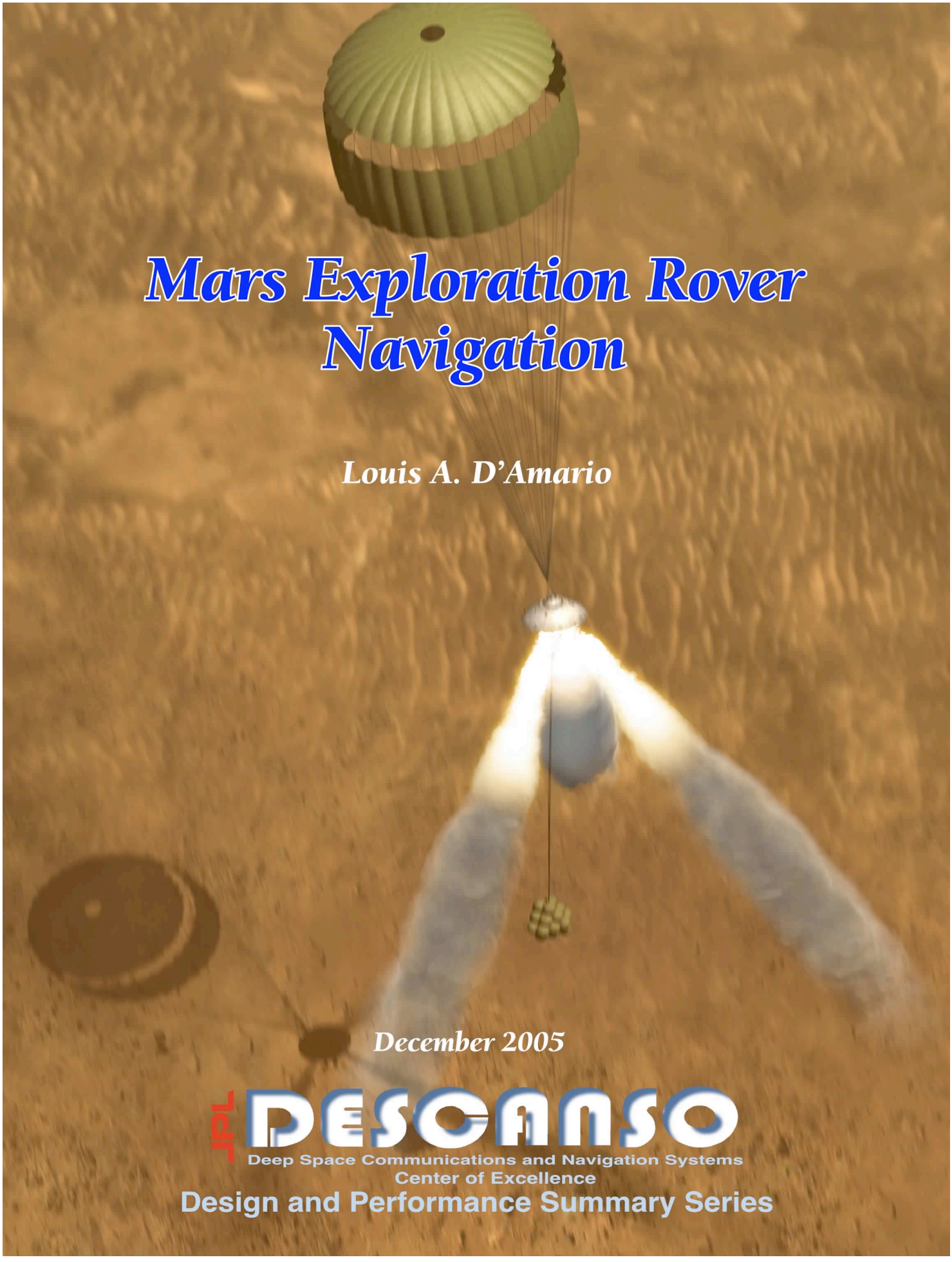

Mars Exploration Rover Navigation

Louis A. D'Amario

December 2005

JPL DESCANSO
Deep Space Communications and Navigation Systems
Center of Excellence
Design and Performance Summary Series

For the picture on the cover:

DESCANSO Design and Performance Summary Series

Article 11

Mars Exploration Rover Navigation

Louis A. D'Amario

Jet Propulsion Laboratory
California Institute of Technology
Pasadena, California

National Aeronautics and
Space Administration
Jet Propulsion Laboratory
California Institute of Technology
Pasadena, California

December 2005

This research was carried out at the
Jet Propulsion Laboratory, California Institute of Technology,
under a contract with the
National Aeronautics and Space Administration.

DESCANSO DESIGN AND PERFORMANCE SUMMARY SERIES

Issued by the Deep Space Communications and Navigation Systems
Center of Excellence
Jet Propulsion Laboratory
California Institute of Technology

Joseph H. Yuen, Editor-in-Chief

Previously Published Articles in This Series

Article 1—"Mars Global Surveyor Telecommunications"
Jim Taylor, Kar-Ming Cheung, and Chao-Jen Wong

Article 2—"Deep Space 1 Telecommunications"
Jim Taylor, Michela Muñoz Fernández, Ana I. Bolea Alamañac, and Kar-Ming Cheung

Article 3—"Cassini Orbiter/Huygens Probe Telecommunications"
Jim Taylor, Laura Sakamoto, and Chao-Jen Wong

Article 4—"Voyager Telecommunications"
Roger Ludwig and Jim Taylor

Article 5—"Galileo Telecommunications"
Jim Taylor, Kar-Ming Cheung, and Dongae Seo

Article 6—"Odyssey Telecommunications"
Andre Makovsky, Andrea Barbieri, and Ramona Tung

Article 7—"Deep Space 1 Navigation: Extended Missions"
Brian Kennedy, Shyam Bhaskaran, J. Edmund Riedel, and Mike Wang

Article 8—"Deep Space 1 Navigation: Primary Mission"
Brian Kennedy, J. Edmund Riedel, Shyam Bhaskaran, Shailen Desai, Don Han, Tim McElrath, George Null, Mark Ryne, Steve Synnott, Mike Wang, and Robert Werner

Article 9—"Deep Impact Flyby and Impactor Telecommunications"
Jim Taylor and David Hansen

Article 10—"Mars Exploration Rover Telecommunications"
Jim Taylor, Andre Makovsky, Andrea Barbieri, Ramona Tung, Polly Estabrook, and A. Gail Thomas

Table of Contents

List of Figures

List of Tables

Foreword

This Design and Performance Summary Series, issued by the Deep Space Communications and Navigation Systems Center of Excellence (DESCANSO), is a companion series to the DESCANSO Monograph Series. Authored by experienced scientists and engineers who participated in and contributed to deep-space missions, each article in this series summarizes the design and performance for major systems such as communications and navigation, for each mission. In addition, the series illustrates the progression of system design from mission to mission. Lastly, it collectively provides readers with a broad overview of the mission systems described.

Joseph H. Yuen
DESCANSO Leader

Acknowledgments

The outstanding MER navigation results presented in this paper are the direct result of the efforts of a large group of people, including the following: Timothy McElrath (orbit determination lead); Christopher Potts (propulsive maneuver analysis lead); Darren Baird, Eric Graat, Brian Portock, and Geoff Wawrzyniak (Orbit Determination [OD] analysis); Behzad Raofi (propulsive maneuver analysis); Julie Kangas (propulsive maneuver and EDL trajectory analysis); Philip Knocke (EDL trajectory analysis lead); Ralph Roncoli and Prasun Desai (EDL trajectory analysis); Lynn Craig (trajectory analysis); Mike Watkins (Navigation and Mission Design Section Manager); Joseph Guinn (orbit determination and rover position determination); Shyam Bhaskaran (test and training); Tomas Martin-Mur (radiometric tracking data processing); Kevin Criddle, Earl Higa, and Neil Mottinger (launch navigation); Laura Campanelli, Lorena Carrillo, K. J. Lee, and Teresa Thomas (radiometric data processing team); Peter Antreasian, Amy Attiyah, and Ron Baalke (OD software development); Brian Kennedy (MarsLS programmer); Victor Legerton (navigation software sub-system engineer); Daniel Lyons (mission design software sub-system engineer); Dimitri Gerasimatos (navigation computing system administrator); Jean Patterson and James Border (ΔDOR team); Moriba Jah and Michael Wilson (off-site backup emergency navigation facility staffing); Walid Majid, Sumita Nandi, and Elizabeth Quintanilla (UHF Doppler processing); and, lastly, the members of the Navigation Advisory Group of the Navigation and Mission Design Section. Special thanks go to Ralph Roncoli who filled in several gaps in the author's incomplete knowledge of certain navigation team activities.

This research was carried out at the Jet Propulsion Laboratory, California Institute of Technology, under a contract with the National Aeronautics and Space Administration.

Reference herein to any specific commercial product, process, or service by trade name, trademark, manufacturer, or otherwise, does not constitute or imply its endorsement by the United States Government or the Jet Propulsion Laboratory, California Institute of Technology.

Mars Exploration Rover Navigation

Louis A. D'Amario[1]
Jet Propulsion Laboratory, California Institute of Technology, Pasadena, California, 91109

The twin Mars Exploration Rovers, *Spirit* and *Opportunity*, were launched on June 10, 2003,[2] and July 8, 2003, from Cape Canaveral, Florida. *Spirit* and *Opportunity* were targeted for landings at Gusev Crater (arrival on January 4, 2004) and Meridiani Planum (arrival on January 25, 2004). The primary navigation challenge was to deliver each spacecraft to the desired atmospheric entry interface point with sufficient accuracy such that each lander would touch down within a specified landing ellipse (about 70 km x 5 km) determined to be safe for landing and also judged to be scientifically interesting. In order to achieve landing within the target ellipse, precise control of the inertial entry flight path angle (FPA) at atmospheric entry was required. The maximum allowable errors in FPA following trajectory correction maneuver (TCM)-5 (trajectory correction maneuver #5) at Entry (E) – 2 days were ±0.12° (3σ) for *Spirit* and ±0.14° (3σ) for *Opportunity*. Achieving these entry delivery accuracies necessitated significant improvements to the interplanetary navigation system used for MER. These improvements included new processes and software for orbit determination, propulsive maneuver design, and entry, descent, and landing (EDL) trajectory simulation. The actual achieved atmospheric entry accuracies for *Spirit* and *Opportunity* significantly exceeded the requirements. At the navigation data cutoff for the TCM-5 final design, the orbit determination FPA knowledge error was ±0.028° (3σ) for *Spirit* and ±0.035° (3σ) for *Opportunity*. Because of exceptionally accurate navigation performance, TCM-5 (E – 2 days) and TCM-6 (E – 4 hours) were canceled for both *Spirit* and *Opportunity*. The actual landing locations (determined from in-situ Doppler tracking between the MER rovers and the Mars Odyssey orbiter) differed from the target landing points by 10.1 km (downtrack) for *Spirit* and 24.6 km (downtrack) for *Opportunity*. The majority of the landing position offsets for both landers was primarily caused by variations in atmosphere and spacecraft aerodynamic modeling from what was predicted. The amount of the landing position offset caused by navigation-only errors was only 3.3 km (uptrack) for *Spirit* and 9.7 km (downtrack) for *Opportunity*.

Nomenclature

ΔV	=	delta velocity
$B \cdot R$	=	component of B-vector (hyperbolic miss vector) along R axis
$B \cdot T$	=	component of B-vector (hyperbolic miss vector) along T axis
C_3	=	square of asymptotic hyperbolic velocity
I_{sp}	=	specific impulse
θ	=	B-plane angle

I. Introduction

THE twin Mars Exploration Rovers, *Spirit* and *Opportunity*, were successfully launched on June 10, 2003,[2] and July 8, 2003, from Cape Canaveral, Florida. *Spirit* (also known as MER-A) was targeted for a January 4, 2004, arrival at Mars. The arrival date for *Opportunity* (MER-B) was exactly three weeks later on January 25, 2004. The landing target for *Spirit* was within Gusev Crater. The target for *Opportunity* was in the Meridiani Planum region, essentially on the opposite side of Mars from Gusev. The primary navigation challenge for the Mars Exploration Rovers (MER) mission was to deliver each spacecraft to the desired atmospheric entry interface point with sufficient accuracy such that each lander would touch down within a specified landing ellipse that was determined to be safe

[1] Principal Member Engineering Staff, Navigation and Mission Design Section, MS 301-125L, Associate Fellow AIAA.
[2] All dates quoted in this report are in Coordinated Universal Time (UTC).

for landing and also scientifically interesting. The dimensions of the landing ellipses for both *Spirit* and *Opportunity* were quite small – i.e., on the order of 70 km (total downtrack) by 5 km (total crosstrack), at the 99% probability level. In order to achieve landing within the target ellipse, precise control of inertial flight path angle (FPA) at atmospheric entry was required. The atmospheric entry interface point was defined to be at a Mars radius of 3522.2 km. The maximum allowable errors in FPA at trajectory correction maneuver (TCM)-5 (trajectory correction maneuver #5) at E – 2 days were ±0.12° (3σ) for *Spirit* and ±0.14° (3σ) for *Opportunity*. These errors are equivalent to a Mars B-plane accuracy of about ±3 km in the B-magnitude direction, which is roughly equivalent to the semi-minor axis (SMIA) of the Mars B-plane error ellipse.

Accomplishing the entry delivery accuracies quoted in the preceding paragraph necessitated significant improvements to the interplanetary navigation system used for MER. These improvements included new processes and software for orbit determination, propulsive maneuver design, and entry, descent, and landing (EDL) trajectory simulation. Orbit determination (OD) enhancements included reexamination of all assumptions used in the baseline OD filter to make them more realistic and eliminate unnecessary conservatism, inclusion of a campaign of frequent delta-differenced one-way ranging (ΔDOR) measurements in the navigation baseline, development of a new OD scripting architecture for automated OD filter processing to enable computation and visualization of numerous solutions using varying OD filter assumptions (up to 50 cases in a single computer run), and development of new software for surface position determination using in-situ Doppler data between MER and the Mars Odyssey (ODY) orbiter. New propulsive maneuver design processes were developed to rapidly evaluate maneuver options for TCM-1 in terms of maneuver epoch, landing target, and maneuver mode, and to evaluate and design propulsive maneuvers for TCMs 4, 5, and 6 to eliminate undesirable maneuver characteristics in terms of the path of the maneuver in the B-plane or on the surface. EDL trajectory simulation was enhanced in order to automate the process of atmospheric entry targeting to achieve a specified landing target, and new software was developed to visualize landing dispersions on Mars surface maps and to evaluate various statistical measures of landing site safety and various science-related factors.

The remainder of this paper addresses the following topics: mission overview, MER spacecraft configuration, key navigation requirements, navigation system, interplanetary cruise navigation, real-time EDL event detection, and rover position determination. Detailed descriptions of the various aspects of MER navigation operations can be found in companion papers [1–9].

II. Mission Overview

The primary objective of the MER Project was to launch two spacecraft to Mars in the 2003 opportunity in order to deliver two surface rovers to different near-equatorial landing sites. During a planned baseline surface mission lasting 91 Martian sols (~93.5 Earth day), each rover would collect data on the composition of targeted Martian soil and rocks and also would provide images and spectra to document the target surroundings and the landing sites. MER-A (carrying the *Spirit* rover) would be launched first during a 21-day launch period extending from May 30, 2003, through June 19, 2003, and it was scheduled to arrive at Mars on January 4, 2004. MER-B (carrying the *Opportunity* rover) would be launched second during a 21-day launch period extending from June 25, 2003, through July 15, 2003, and it was scheduled to arrive at Mars on January 25, 2004.

Both MER flight systems were interchangeable and consisted of a cruise stage, an EDL system (including heatshield, backshell, parachute, retro-rockets, airbags and lander structure), and a rover, which was enclosed inside the lander.

During the approximately 7-month interplanetary transfer for each spacecraft, which included the cruise and approach (starting at E – 45 days) mission phases, six TCMs were planned to deliver each flight system to the specified Mars atmospheric entry aimpoint. In addition, during the cruise phase, telecom, navigation, and rover instrument checkouts were performed. The EDL phase began at the atmospheric entry interface point. Telecommunications during the interplanetary phase was accomplished via a low gain antenna (LGA) and a medium gain antenna (MGA) using an X-band link.

EDL adapted the concept developed for Mars Pathfinder: first employing a heatshield and a parachute to slow descent through the Martian atmosphere, then firing retro-rockets to reduce landing speed, and finally utilizing airbags to cushion surface impact. After the airbag assembly rolled to a stop, the system retracted the airbags, opened the three lander petals while righting the landing structure, and prepared the rover to leave the lander. Both landers touched down early in the Martian afternoon while the Earth was still in view, allowing the transmission of multiple-frequency shift key (M-FSK) tones, which are coded to indicate completion of critical events during EDL. After landing, the *Spirit* and *Opportunity* rovers began their 91-sol surface operations phase. The desired landing site for *Spirit* was inside Gusev Crater at 14.59° south latitude and 175.30° east longitude. The landing site for

Opportunity was in the Meridiani Planum region at 1.98° south latitude and 354.06° east longitude. (Latitude and longitude are specified with respect to the International Astronomical Union/International Association of Geodesy [IAU/IAG] 2000 system.[9]) The Earth range at arrival was 1.14 AU for *Spirit* and 1.33 AU for *Opportunity*.

Each Rover used five science instruments to record data about the landing sites and selected rock and soil targets. The science payload consisted of two remote sensing instruments and three instruments for in-situ observations. The two remote sensing instruments were the Stereo Panoramic Imager (Pancam) and the Miniature Thermal Emission Spectrometer (Mini-TES). The three in-situ instruments were the Mössbauer Spectrometer, the Alpha-Particle X-Ray Spectrometer (APXS), and the Microscopic Imager. Along with the three in-situ instruments, a fourth device, called the Rock Abrasion Tool (RAT), was mounted on the end of the 5 degree-of-freedom (DOF) Instrument Deployment Device (IDD) arm. The RAT was used to remove the outer surfaces of rocks to allow analysis of the freshly exposed, less-weathered material.

The rovers were designed to be capable of traveling over 40 m in a single sol and accomplishing a total traverse distance during the surface mission of at least 600 m. Science data were returned to Earth via either a direct-to-Earth (DTE) X-band link from the rover, using an LGA and a high gain antenna (HGA) or via a ultra high frequency (UHF) link to the ODY or Mars Global Surveyor (MGS) orbiters, using a UHF antenna.

III. MER Spacecraft Configuration

A. Structure and Components

Figure 1 shows a breakdown of the MER flight system, and Fig. 2 shows a more detailed view of spacecraft in cruise configuration. The design of the MER flight system was an adaptation of the Mars Pathfinder spacecraft design. As such, during flight, MER was a spin-stabilized spacecraft with a nominal spin rate of 2 rpm. The MER flight system consisted of four major components: the cruise stage, the EDL system (or aeroshell) consisting of a heatshield and a backshell, the lander, and the rover. The mass allocation for the entire flight system (including propellant) was 1077.0 kg. The actual launch masses (including a full 52.0 kg propellant load) were 1061.6 kg for *Spirit* and 1064.4 kg for *Opportunity*.

The cruise stage included solar panels, the propulsion system, which included two propellant tanks and two

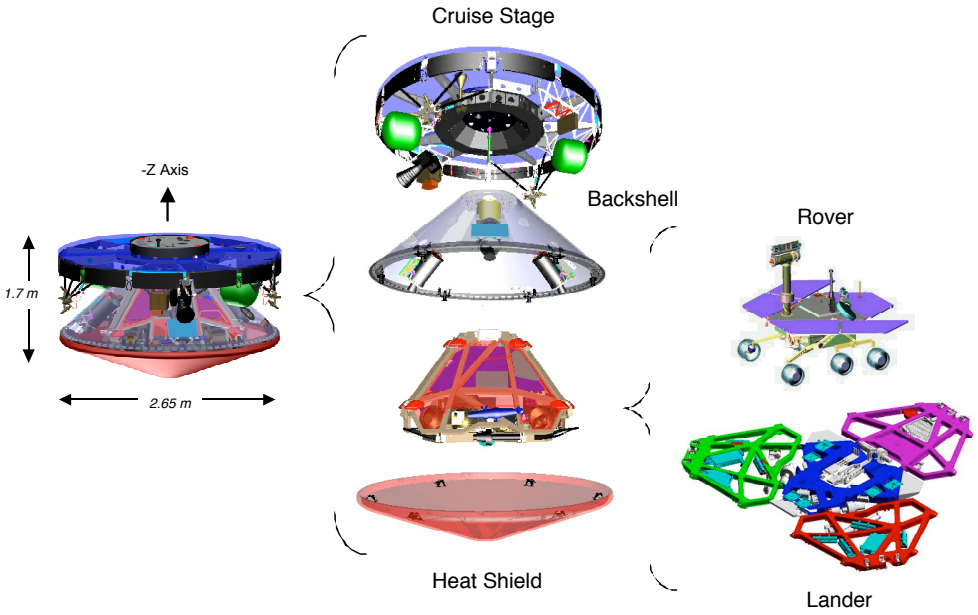

Figure 1: MER flight system breakdown.

thruster clusters, the attitude control system (ACS), which included a star scanner, inertial measurement unit (IMU), Sun sensors, and an LGA and an MGA for X-band communications with Earth. Both antennas were oriented in the spacecraft –Z direction. The cruise stage was separated from the backshell/heatshield assembly 15 minutes prior to entry.

During the interplanetary transfer to Mars, the lander structure (containing the rover) was enclosed by the backshell/heatshield assembly, which is also referred to as the aeroshell. The aeroshell protected the lander and rover from extreme heat loads experienced during atmospheric entry. The heatshield thermal protection system dissipated energy as the spacecraft entered the Martian atmosphere. The backshell included the parachute canister and rocket assisted deceleration (RAD) motors, both of which were used to slow the Lander prior to touchdown on the surface. The backshell also included an aft-mounted LGA for X-band communications during EDL.

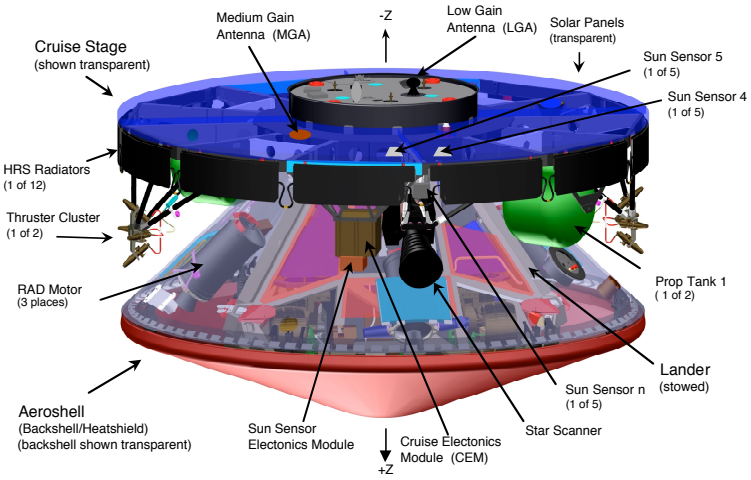

Figure 2: MER spacecraft in cruise configuration.

The lander structure enclosed the rover and included the lander petals, the rover deployment mechanism, the airbag system, the radar altimeter, the batteries, and an LGA antenna. The rover included the science instruments, the solar arrays, the batteries, a UHF antenna for the relay link to the ODY or MGS orbiters, and an X-band telecom system for communications with Earth. The X-band system consisted of an LGA, HGA, small deep-space transponder (SDST) and redundant solid-state power amplifiers (SSPAs). Much of the electronics that perform spacecraft functions (including during interplanetary cruise) were contained on the rover.

B. Propulsion System

The MER propulsion system included the hardware needed to perform spin and attitude control and TCMs during interplanetary cruise and approach. The propulsion system hardware, located on the cruise stage, was a monopropellant hydrazine system that operated in a 3:1 blowdown range. The propellant system consisted of two hydrazine tanks, line feeds and filters, two latch valves, and eight thrusters in two clusters of four thrusters each (see Fig. 3).

The hydrazine propellant was contained in two 42-cm diameter composite-overwrapped propellant tanks that were pressurized with helium at an initial tank pressure of 350 psia (2.413 MPa). At launch, these tanks were loaded with 52 kg of propellant. The thrusters each produced approximately 4.6 N thrust at the initial tank pressure of 350 psia (2.413 MPa); at end of life, each thruster produced approximately 1.8 N thrust at a residual pressure of 117 psia (0.807 MPa).

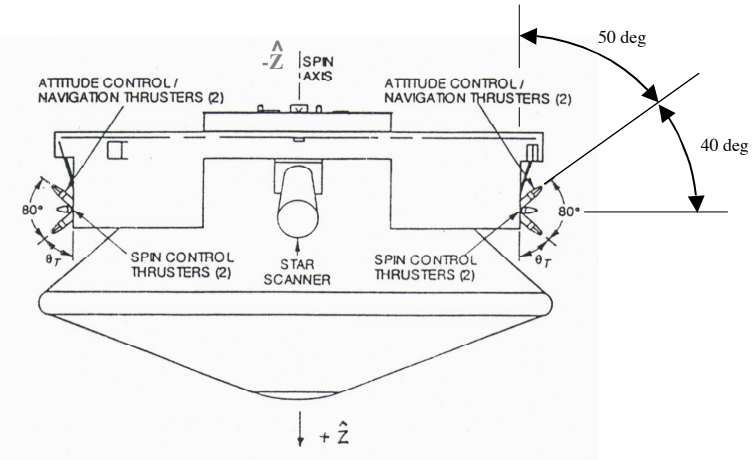

Figure 3: Spacecraft thruster configuration.

The thruster cluster assemblies were diametrically opposed. On one side of the spacecraft, thrusters 1 through 4 were aligned 40° off the –X axis; that is, starting from a –X orientation, the thrusters were pointed 40° toward the +Z direction and 40° toward the –Z direction in the X-Z plane and 40° toward the +Y direction and 40° toward the –Y direction in the X-Y plane. Thrusters 5 through 8 were aligned 40° off the +X axis in a similar fashion on the opposite side of the spacecraft.

For performing TCMs, an axial burn imparts a velocity change (ΔV) in the +Z or –Z direction (i.e., along the spin axis). Axial burns were performed by firing pairs of thrusters in steady state mode. The desired ΔV for an axial burn was achieved by firing the thrusters for a specified amount of time. A lateral burn imparts a ΔV in a direction approximately normal to the spin axis. The spacecraft rotated at 2 rpm about the +Z axis. At the appropriate

orientation in the spin cycle, the four thrusters of one thruster cluster were each fired typically for 5 seconds; this provided one pulse of lateral ΔV. Fifteen seconds later (one-half revolution), the other cluster's four thrusters were each fired for 5 seconds (another pulse). Because the spacecraft's center of mass was located further along the +Z axis than the thruster clusters, the two thrusters (one per cluster) that provided ΔV in the –Z direction were fired for a shorter duration than 5 seconds. This caused the net thrust from firing each cluster's four thrusters to point through the spacecraft center of mass, thereby eliminating attitude perturbations. The desired ΔV for a lateral burn was achieved by repeating this process for a specified number of pulses. Spacecraft attitude maneuvers (turns) and spin-rate control were accomplished by pulse-mode firing of coupled thruster pairs. There were two sets of thruster pairs that were used for these maneuvers.

The cant angles of the thrusters caused burn losses for both axial and lateral maneuvers. The thrusters used for axial maneuvers were canted 50° away from the spin axis of the spacecraft, causing inefficiencies or burn losses of 55.6% (one divided by the cosine of 50°). For lateral maneuvers, the thrusters were canted 40° away from the lateral direction, causing burn losses of 30.5% (one divided by the cosine of 40°). In addition, lateral maneuvers had a 4.7% burn loss caused by the finite 60° (5-second) burn arc used for a pulsing the lateral thrusters. The total burn loss for lateral maneuvers was thus 36.7% (1.305 x 1.047). Because of their smaller total burn losses, lateral maneuvers were more efficient than axial maneuvers in terms of propellant usage.

The I_{sp} values were nominally 222.2 seconds for axial burns and 221.4 seconds for lateral burns. These values represented the average I_{sp} for the entire interplanetary cruise, taking into account the variation of I_{sp} with tank pressure, and they had also been adjusted to take into account plume impingement losses: 2% for the four –Z and +Z facing thrusters and 1% for the remaining four thrusters.

C. Telecommunications System

The MER telecommunications subsystem used X-band for DTE communications during all mission phases and a UHF system during both EDL (after bridle deployment) and on the surface of Mars for relay communications through the ODY and MGS orbiters.

The X-band telecommunications system design was single-string coherent X-Band Uplink/X-Band Downlink with electronics located in the rover. The same X-band electronics were used from launch through end of mission, but four different sets of X-band antennas were required: an MGA-LGA pair on the cruise stage for communications during interplanetary flight, a backshell-mounted LGA to support communications during EDL, one small patch LGA on the lander base petal to support communications after landing and prior to rover deployment, and an HGA-LGA pair on the rover for surface operations.

The single-string UHF equipment was also in the rover and was used with two different antenna sets: a UHF antenna mounted on the lander structure to support communications during EDL and a UHF antenna mounted on the rover for surface communications.

The X-band telecommunications equipment included an SDST and two SSPAs, all located in the rover. The heart of the X-band telecommunications system was the SDST, which supported phase coherent turn-around Doppler and ranging, command signal demodulation and detection, telemetry coding and modulation, and DOR tone generation (at ±19 MHz).

IV. Key Navigation Requirements

The key requirements on navigation can be divided into the following areas: planetary protection, TCM ΔV and propellant, atmospheric entry delivery accuracy, real-time EDL event detection, and rover position determination. The requirements are listed in the following sections along with brief comments relating to satisfaction of the requirements.

A. Planetary Protection

1. The probability of impact of Mars by the launch vehicle upper stage shall be less than 1.0×10^{-4}.
2. The probability of non-nominal impact of Mars due to failure during the cruise and approach phases shall not exceed 1.0×10^{-2}.

The launch vehicle upper stage impact probability requirement was satisfied by biasing the launch vehicle injection aimpoint away from Mars. This caused TCM-1 to have a deterministic component. No special actions were required to satisfy the non-nominal impact requirement. The value for non-nominal impact probability was recalculated whenever the TCM strategy or delivery accuracy capabilities changed to verify that the requirement was still satisfied. The strategies for satisfying the planetary protection requirements are also discussed in [4 and 5].

B. TCM ΔV and Propellant

1. Delivery to the desired atmospheric entry conditions shall be accomplished with a probability of 99% with respect to available propellant.
2. TCM propellant requirements shall be determined such that there is sufficient propellant with 90% probability for a TCM-1 delayed until launch plus 30 days.

Satisfaction of these requirements was monitored closely during the development phase prior to launch, since the projected available propellant load did not provide large propellant margins. Extremely accurate launch vehicle injection performance rendered these requirements moot during flight operations. The analyses used to demonstrate satisfaction of these requirements are discussed in [5].

C. Atmospheric Entry Delivery Accuracy

1. The MER-A (*Spirit*) and MER-B (*Opportunity*) interplanetary trajectories shall be targeted to an inertial atmospheric entry FPA of –11.5° with a 3-sigma TCM-5 delivery uncertainty of less than ±0.12° for Gusev Crater and ±0.14° for Meridiani Planum.

This requirement was, arguably, the single most important requirement levied on navigation. Atmospheric entry delivery accuracy directly affected the size of the landing ellipse, and thus it represented an important factor in the determination of acceptable landing sites. This requirement was effectively driven by navigation capabilities. As a result, it was changed as navigation capabilities improved. The FPA delivery errors listed here represent the values in effect prior to the final approach TCMs. Actual navigation performance exceeded these requirements by a wide margin as described in subsequent sections of this paper and in [1].

D. Real-time EDL Event Detection

1. The navigation system shall provide the capability to process and evaluate DTE X-band one-way Doppler data during final approach and EDL to attempt real-time confirmation of the following events: turn to entry attitude, cruise stage separation, atmospheric deceleration, and parachute deployment.

Prior to launch, it was not known whether this requirement could be satisfied, although experience from Mars Pathfinder indicated that successful detection of these EDL events was likely. These processes and results for successful real-time EDL event detection are described in a subsequent section of this paper and also in [6].

E. Rover Position Determination

1. The areocentric location of each landing site (using IAU 2000 coordinate system definitions) shall be determined to a 3-sigma accuracy of 10 km within 5 sols of landing.
2. The areocentric location of each landing site (using IAU 2000 coordinate system definitions) shall be determined to a 3-sigma accuracy of 100 m within 3 sols of landing, given that the rover has not moved more than 10 m from the landing site during this time.
3. The areocentric location of each rover (using IAU 2000 coordinate system definitions) shall be determined to a 3-sigma accuracy of 30 m, given that the rover has not moved more than 3 m for at least 3 sols.

The first requirement assumes the use of DTE X-band Doppler only for determining the landing location; the second assumes use of both DTE X-band and in-situ UHF Doppler between the rover and the Odyssey orbiter. Determining the landing location of each rover using radiometric data was a high-priority activity, because it could have been important in selecting the direction in which each rover would drive once it departed the landing site in the event that determining the landing location using landmark triangulation had been judged unreliable. Prior to MER, surface position determination using in-situ surface-to-orbiter Doppler data in combination with DTE Doppler data had never been attempted. Pre-arrival analyses indicated that these requirements could be met. Following landing, the surface positions of both *Spirit* and *Opportunity* were determined within the required accuracy. The results are given in a subsequent section of this paper.

V. Navigation System

The navigation system consists of three general functional elements: orbit determination (includes rover position determination), propulsive maneuver design and analysis, and EDL trajectory design and analysis. Navigation functions during MER flight operations included the following:

1. Process radiometric tracking data (Doppler, range, and ΔDOR) to solve for the spacecraft trajectory and associated uncertainties.
2. Perform EDL trajectory analysis to determine desired atmospheric entry aimpoints for TCMs and to evaluate landing dispersions and related metrics for landing success.

3. Perform EDL trajectory analysis to provide inputs for uplink of EDL parameter updates.
4. Determine the desired ΔV vector for TCMs to achieve the specified atmospheric entry aimpoint and verify the TCM implementation provided by the spacecraft team.
5. Process MER and Mars Odyssey radiometric tracking data to estimate the rover position and associated uncertainties.
6. Generate spacecraft ephemeris files and ancillary trajectory data products.
7. Provide real-time monitoring during TCMs and reconstruct the TCM ΔV using pre- and post-TCM tracking data.

The reminder of this section describes the models and processes used for navigation analysis.

A. Navigation Data Types

The baseline radiometric data types used for orbit determination were two-way coherent Doppler, two-way coherent ranging, and ΔDOR measurements. Doppler and range are traditional data types derived from the coherent X-band radio link between the spacecraft and a receiver at a Deep Space Network (DSN) ground station. Doppler data provide a measurement of the line-of-sight spacecraft range rate based on Doppler frequency shift. Range data provide an estimate of the range to the spacecraft by measuring the round-trip light time of a radio signal between a DSN station and the spacecraft. The Doppler accuracy observed in flight was typically 1 – 2 mHz (1σ), which is equivalent to 0.015 – 0.035 mm/s (1σ). Range accuracy was typically on the order of 1 m (1σ) for a 10-minute integration time. The observed accuracies exceeded pre-launch assumed values by better than a factor of two for Doppler and by about a factor of four for range.

ΔDOR measurements were acquired by having two DSN stations simultaneously observe the spacecraft followed by simultaneous observations of a reference radio source (quasar). ΔDOR measured the angular separation between the spacecraft and the quasar. The two possible pairings of DSN stations were Goldstone–Madrid and Goldstone–Canberra. The Goldstone–Madrid baseline (oriented east–west) primarily measured the right ascension component of the spacecraft, whereas the Goldstone–Canberra baseline (oriented north–south) primarily measured the declination component. ΔDOR complements Doppler and range measurements because of its orthogonality to those data types. ΔDOR measurements also are independent of geometry and do not rely on dynamic models to infer position (unlike Doppler and range). The ΔDOR observable was a phase delay time expressed in units of nanoseconds (ns) that is equivalent to an angular separation between the spacecraft and the quasar. ΔDOR accuracy was typically about 0.04 ns, which is equivalent to 1.5 nanoradians (nrad). This was about a factor of three better than pre-launch assumptions.

B. DSN Navigation Tracking Coverage

DSN navigation tracking coverage (Doppler, range, and ΔDOR) for *Spirit* and *Opportunity* was baselined using the 34-meter high efficiency (HEF) subnet. For particular activities (e.g., TCMs), and for EDL, coverage was provided by 70-meter antennas. Following launch, both spacecraft utilized the cruise stage LGA for communications. At 59 days from launch (August 8, 2003) for *Spirit* and 37 days from launch (August 14, 2003) for *Opportunity*, communication was switched to the cruise stage MGA. The navigation tracking coverage requests for *Spirit* and *Opportunity* are shown in Tables 1 and 2. The Doppler and range coverage for *Opportunity* was slightly reduced (as compared to *Spirit*) for the period from E – 45 days to E – 35 days, because of the overlap of the *Spirit* and *Opportunity* approach phases. There were no differences between *Spirit* and *Opportunity* with respect to the requested frequency of ΔDOR measurements.

Table 1: *Spirit* DSN navigation tracking request.

Doppler and Range Coverage				
Start	End	Start	End	DSN Request
Launch	L + 30	6/10/03	7/10/03	Continuous
L + 30	E – 45	7/10/03	11/20/03	3 tracks/week
E – 45	E – 21	11/20/03	12/14/03	~2.5 tracks/day
E – 21	Entry	12/14/03	1/4/04	Continuous

Frequency of ΔDOR Measurements				
Start	End	Start	End	DSN Request
L + 21	E - 45	7/1/03	11/20/03	1/week
E - 45	E - 28	11/20/03	12/7/03	2/week
E - 28	E - 8	12/7/03	12/27/03	1 every other day
E - 8	Entry	12/27/03	1/4/04	1/day

Table 2: *Opportunity* DSN navigation tracking request.

Doppler and Range Coverage				
Start	End	Start	End	DSN Request
Launch	L + 30	7/8/03	8/7/03	Continuous
L + 30	E – 45	8/7/03	12/11/03	3 tracks/week
E – 45	E – 35	12/11/03	12/21/03	~2 tracks/day
E – 35	E – 21	12/21/03	1/4/04	~2.5 tracks/day
E – 21	Entry	1/4/04	1/25/04	Continuous

Frequency of ΔDOR Measurements				
Start	End	Start	End	DSN Request
L + 21	E - 45	7/29/03	12/11/03	1/week
E - 45	E - 28	12/11/03	12/28/03	2/week
E – 28	E – 8	12/28/03	1/17/04	1 every other day
E - 8	Entry	1/17/04	1/25/04	1/day

Overall, DSN performance during interplanetary cruise was excellent. Loss of entire tracks of Doppler and range data was rare. When this did occur, it was usually caused by DSN equipment problems or by deliberate sacrificing of tracking passes to provide additional coverage to the other MER spacecraft or to another mission. Occurrences of degraded tracking data during a pass, as evidenced by anomalous signatures or biases in Doppler or range data, were experienced, especially early in interplanetary cruise. These problems were most often caused by DSN procedural problems, such as missing or incorrect calibrations, incorrect configuring of DSN equipment (e.g., uplink signal polarization), or use of incorrect predicts. Severe solar flares that occurred during interplanetary cruise also caused degraded Doppler and range accuracy. Particular problems were noted with DSS-26 relating to incorrect z-height calibration and a significant error in the station location. Both of these problems were corrected. Near the beginning of the approach phase for *Spirit* (November 20, 2003), the DSN had been sensitized to tracking data issues caused by procedural problems and their possible negative impact on MER navigation performance, and the rate of tracking data anomalies was significantly reduced.

The performance of the ΔDOR system was exceptional. The total number of ΔDOR measurements attempted was 131. There were 64 measurements attempted for *Spirit* and 67 for *Opportunity*. There were only three failures; this translates to a success rate of 98%. Many of the ΔDOR measurements were dual-spacecraft measurements that provided ΔDOR data points for both *Spirit* and *Opportunity*. This effectively increased the total number of measurements above that indicated in Tables 1 and 2. By the final approach phase, the processing time for ΔDOR measurements, which is defined as the total time from recording of raw data to delivery of a tracking data file to the Radiometric Data Conditioning (RMDC) group, had been reduced to 8 hours or less. The largest amount of this time was for playback and transmission to JPL of data recorded during the measurement.

C. OD Filter Configuration

The OD process used a least-squares batch estimation filter. The filter minimized tracking data residuals over the data arc in order to estimate the state (position and velocity) of the spacecraft at a specified epoch (usually the start of the data arc) and any other parameters included in the estimation list. The filter also output the uncertainties in the estimated parameters. Parameters that are not estimated, but whose a priori uncertainties are incorporated in the results, are called consider parameters.

The OD filter configuration used just prior to launch for final OD covariance studies is shown in Table 3. The OD filter configuration used during final approach navigation operations is shown in Table 4. Between launch and final approach, experience with tracking data, OD solutions, and other factors caused changes to the baseline OD filter configuration. The high quality of Doppler, range, and ΔDOR data obtained during navigation operations enabled reductions in their a priori uncertainties. Similarly, favorable results from the ACS/NAV calibrations (see Section VI) for both spacecraft allowed significant reductions in the ACS event ΔV uncertainties, and actual spacecraft TCM performance permitted reductions in the assumed values for maneuver execution errors. The stochastic nongravitational acceleration model was eliminated from the filter in favor of upgrades to the solar

Table 3: OD filter configuration – pre-launch.

Error Source	Estimated?	A Priori Uncertainty (1σ)	Correlation Time	Update Time	Comments
2-way Doppler (mm/s)	–	0.075	–	–	~4.5 mHz
Range (m)	–	4	–	–	29 range units
ΔDOR (nrad)	–	4.5	–	–	0.12 ns
Epoch State					
Position (km)	✓	1000	–	–	
Velocity (km/s)	✓	1	–	–	
Solar Pressure					Sunlit area of spacecraft.
Area (%)	✓	5	–	–	
Specular & Diffuse Coefficients (%)	✓	10	–	–	
ACS Event ΔV (mm/s)					Every 8 days.
Line-of-Sight Comp.	✓	3	–	–	
Lateral Comp.	✓	3	–	–	
Normal Comp.	✓	3	–	–	
TCMs					MER-A, MER-B respectively
TCM-1	✓	422, 440	–	–	Spherical uncertainty (mm/s)
TCM-2	✓	17, 15	–	–	
TCM-3	✓	3, 5	–	–	TCM-4 at E - 8 days TCM-5 at E - 2 days TCM-6 at E - 6 hours
TCM-4	✓	3, 3	–	–	
TCM-5	✓	3, 3	–	–	5% (3σ) proportional error (per axis) 6 mm/s (3σ) fixed error (per axis)
TCM-6	✓	7, 7	–	–	
Nongravitational Accelerations (km/s^2)	✓	2.0×10^{-12}	10 days	1 day	Spherical covariance; estimated daily (1 day batches).
Range Bias (m)	✓	2	0	Per pass	Estimated per pass.
Doppler Bias (mm/s)	✓	0.005	0	Per pass	Estimated per pass.
Mars & Earth Ephemerides	–	DE405+	–	–	
Station Locations (cm)	–	3	–	–	
Quasar Locations (nrad)	–	2	–	–	
Pole X, Y (cm)	✓	2 – 10	0	6 hours	*Use lower value up to 7 days before data cutoff; ramp up to higher value at data cutoff. (UT1: 0.256 ms = ~10 cm.)
UT1 (cm)	✓	2 – 10	0	6 hours	
Ionosphere – day (cm)	✓	55	0	6 hours	S-band values.
Ionosphere – night (cm)	✓	15	0	6 hours	
Troposphere – wet (cm)	✓	1	0	6 hours	
Troposphere – dry (cm)	✓	1	0	6 hours	

pressure model. The recommended uncertainties for the Mars ephemeris[3] and Earth orientation parameters (EOP)[4] were updated. Additionally, new solutions were delivered for station locations and their uncertainties.[5] Finally, the Doppler bias model was eliminated, because the observed biases were very small, and the updated station locations further decreased the usefulness of including a Doppler bias in the filter model. Overall, during navigation operations, orbit determination performance improved significantly from that based on pre-launch covariance studies. The OD filter strategy and system modeling are discussed in detail in [2 and 3]. OD performance during interplanetary cruise is the subject of [1].

[3] Standish, E. M., *Recommendation of DE410 for MER and Cassini*, JPL D-33747 (JPL internal document), Jet Propulsion Laboratory, Pasadena, California, November 3, 2003.
[4] Ratcliff, J. T., *KEOF Operational EOP Deliveries During MER*, JPL D-33745 (JPL internal document) , Jet Propulsion Laboratory, Pasadena, California, July 24, 2003.
[5] Folkner, W. M. and Jacobs, C. S., *DSN Station Location Update for MER*, JPL D-33746 (JPL internal memo), Jet Propulsion Laboratory, Pasadena, California, November 4, 2003.

Table 4: OD filter configuration – final approach.

Error Source	Estimated?	A Priori Uncertainty (1σ)	Correlation Time	Update Time	Comments
2-way Doppler (mm/s)	–	Weight by pass: ≥0.05	–	–	3.36 x RMS (60 sec) of pass-through residuals. (1.0 mm/s = ~0.056 Hz.)
Range (m)	–	Weight by pass: ≥0.14	–	–	2.22 x RMS of pass-through residuals. (1.0 m = ~7.0 RU.)
ΔDOR (nrad)	–	~3.2	–	–	0.085 ns
Epoch State					
Position (km)	✓	100,000	–	–	Effectively infinite.
Velocity (km/s)	✓	1.0	–	–	Effectively infinite.
Solar Pressure					
Specular Coefficients	✓	0.05	–	–	All components; 0.1 in normal units.
Diffuse Coefficients	✓	0.033			All components; 0.1 in normal units.
Solar Array Diffuse Coef.	✓	0.033	7 days	1 day	Correlation broken at turns.
ACS Event ΔV (mm/s)					
Line-of-Sight Comp.	✓	0.05, 0.1	–	–	MER-A & MER-B values respectively, based on results of ACS/NAV calibration. Location per current plan; all future events included.
Lateral Comp.	✓	0.05, 0.05	–	–	
Normal Comp.	✓	0.05, 0.05	–	–	
TCM-4					
Magnitude (%)	✓	1.67	–	–	Equivalent to 0.127 N.
Pointing (deg)	✓	0.5	–	–	Use 0.5 deg for both cone and clock.
Nongravitational Accelerations (km/s^2)	–	–	–	–	No longer used – accounted for in solar pressure uncertainties and modeling of ACS turns as discreet events.
Charged Particle Effects					
Delay (m)	✓	1.5	–	1 day	
Delay Rate (m/s)	✓	0.00005	–	1 day	Equivalent to ~4 meters per day
Range Bias (m)	✓	2	0	Per pass	Estimated per pass.
Doppler Bias (mm/s)	–	–	–	–	No longer used.
Mars & Earth Ephemerides	–	DE410	–	–	0.5 x DE405+; Mars RTN 1σ Uncertainties: 9 m, 136 m, 442 m.
Station Locations (cm)	–	Per covariance.	–	–	Use latest updates to station locations and covariance.
Quasar Locations (nrad)	–	2	–	–	
Pole X, Y (cm)	✓	1, 4	2 days	6 hours	Use larger value for last 2 – 6 days per Ratcliff document (footnote 4). (For UT1, 0.256 ms ⇒ ~10 cm.)
UT1 (cm)	✓	1.7, 9	2 days	6 hours	
Ionosphere – day (cm)	✓	55, 300	6 hours	1 hour	Subsequent passes uncorrelated; use larger values (6X) for ionosphere when only predicted calibrations available. S-band units.
Ionosphere – night (cm)	✓	15, 100	6 hours	1 hour	
Troposphere – wet (cm)	✓	1, 1	6 hours	1 hour	
Troposphere – dry (cm)	✓	1, 1	6 hours	1 hour	

D. TCM Profile

In order to meet the requirements for Mars atmospheric entry delivery accuracy, a series of six TCMs were planned during the cruise and approach phases of the mission. Tables 5 and 6 show the name, relative time, date, OD data cutoff time, and maneuver objective for each TCM for *Spirit* and *Opportunity*. The locations of the TCMs were chosen as a compromise between the following competing requirements:

1. Provide sufficient time between launch and TCM-1 for spacecraft checkout and design of TCM-1.
2. Provide sufficient time between TCMs to allow for TCM reconstruction, orbit determination, and design and sequence generation for the upcoming TCM.
3. Minimize operational complexity.
4. Minimize Mars atmospheric entry delivery errors.
5. Minimize total mission propellant usage.

There were three TCMs planned during the final approach phase: TCMs 4, 5, and 6. These maneuvers adjusted the trajectory to the desired atmospheric entry conditions. TCM-5 at E – 2 days was nominally the final entry targeting maneuver for landing site safety. In other words, TCM-5 was the last maneuver required to achieve the entry FPA delivery accuracy requirements. TCM-6 at E – 4 hours was the final opportunity to perform a TCM. TCM-6 was included primarily to protect against a late OD error that might be uncovered only when the gravity of Mars began to affect the trajectory. Even though TCM-6 was judged to be extremely unlikely, it was treated and

Table 5: *Spirit* TCM profile.

TCM	Time*	Date	OD Data Cutoff	Description
A1	L + 10 d	6/20/03	TCM – 5 d	Correct injection errors; remove injection bias.
A2	L + 52 d	8/1/03	TCM – 5 d	Correct TCM-A1 delivery errors; target to entry aimpoint.
A3	E – 50 d	11/14/03	TCM – 5 d	Correct TCM-A2 delivery errors.
A4	E – 8 d	12/27/03	TCM – 13 h	Correct TCM-A3 delivery errors.
A5	E – 2 d	1/2/04	TCM – 13 h	Nominal final entry targeting maneuver.
A6	E – 4 h	1/4/04	TCM – 4.6 h	Contingency opportunity for final maneuver.

*Time measured from launch (L) or entry (E).

Table 6: *Opportunity* TCM profile.

TCM	Time*	Date	OD Data Cutoff	Description
B1	L + 10 d	7/18/03	TCM – 5 d	Correct injection errors; remove injection bias.
B2	L + 62 d	9/8/03	TCM – 5 d	Correct TCM-B1 delivery errors; target to entry aimpoint.
B3	E – 65 d	11/21/03	TCM – 5 d	Correct TCM-B2 delivery errors.
B4	E – 8 d	1/17/04	TCM – 13	Correct TCM-B3 delivery errors.
B5	E – 2 d	1/23/04	TCM – 13 h	Nominal final entry targeting maneuver.
B6	E – 4 h	1/25/04	TCM – 4.6 h	Contingency opportunity for final maneuver.

*Time measured from launch (L) or entry (E).

prepared for in exactly the same manner as the other approach-phase maneuvers. The TCM times listed in Tables 5 and 6 are the final execution times (or planned execution times) and reflect re-planning that occurred during flight operations.

The OD data cutoff was 5 days prior to execution for TCMs 1 through 3, 13 hours prior to execution for TCMs 4 and 5, and just 4.6 hours prior to TCM-6 execution. The data cutoff for the final three TCMs was closer to the TCM execution in order to reduce navigation tracking data latency, thereby improving entry delivery accuracy. For TCM-6, the TCM development time was compressed to 4.6 hours in order to include the latest possible navigation tracking data in the orbit determination solution supporting design of the TCM. All TCMs utilized the so-called Auto-TCM behavior. The commands to execute the TCM were part of flight software that was loaded prior to launch. The ground TCM design process determined a set of parameters that governed the execution of the TCM, and these parameters were uplinked to the spacecraft prior to scheduled execution. (The Auto-TCM behavior also included logic that can detect faults and, after recovery from the fault, resume execution of the TCM.)

E. Propulsive Maneuver Modes

Propulsive maneuvers (TCMs) were accomplished using the Auto-TCM behavior in flight software. The Auto-TCM behavior was constructed with the following sequence of five maneuver components: turn, burn, turn, burn, and turn. A turn could be a real turn that reorients the spacecraft spin axis, or it could be a null turn that simply reinforces the current attitude. All turns were balanced – i.e., there is nominally zero ΔV imparted to the spacecraft by the turn. A burn could be an axial burn, a lateral burn, or a null burn (zero commanded ΔV). Thus, the Auto-TCM behavior allowed a great deal of flexibility in the implementation of a propulsive maneuver.

The propulsive maneuver implementation modes considered by MER navigation were the following: *turn and axial burn*, *turn and lateral burn*, *turn and vector mode* (i.e., a turn followed by axial and lateral burns), and *vector mode (no turn)* (i.e., axial and lateral burns performed without a turn). In order to perform a *turn and axial burn* maneuver, the spacecraft spin axis was reoriented such that it was aligned with the desired ΔV and then an axial burn (in either the +Z or –Z direction) was performed. In order to perform a *turn and lateral burn* maneuver, the spacecraft spin axis was reoriented such that it pointed at the proper angle (approximately 98°) relative to the lateral ΔV direction and then a lateral burn was performed. The spin axis could be oriented anywhere (within applicable pointing constraints) on a cone at an angle of approximately 98° from the desired ΔV direction. This angle was determined by the requirement to have the thrust vector point through the spacecraft center of mass such that no net toque was imparted to the spacecraft. For a lateral burn, the thrusters were fired at the appropriate clock angle to provide ΔV in the desired direction. For a *turn and vector mode* maneuver, the spacecraft spin axis was reoriented to a specified attitude and then axial and lateral burns were performed such that the vector addition of the axial and lateral ΔV vectors summed to the desired ΔV. The direction of the spin axis could be chosen to minimize the sum of the magnitudes of the axial and lateral ΔV components. A *vector mode (no turn)* maneuver was similar to a *turn and vector mode* maneuver except the spacecraft orientation was not changed.

With the exception of TCM-1, all TCMs were accomplished as vector mode (no turn) maneuvers. The reason was that, based on pre-launch analyses, TCM-1 could have had a large maneuver magnitude and, in order not to exceed available propellant, multiple maneuver implementation modes were allowed to minimize propellant consumption. All TCMs following TCM-1 were much smaller in magnitude and could be accomplished with a vector mode maneuver (no turn) implementation at the nominal cruise attitude without incurring large propellant penalties.

F. Propulsive Maneuver Constraints

During flight operations, there were certain spacecraft pointing limitations in effect for TCM-1 that constrained the available attitudes at which the maneuver could be performed. In order to provide desired telecom performance, the off-Earth angle of the spacecraft –Z axis could not exceed 90°. In order to provide sufficient electrical power from the solar arrays and maintain spacecraft temperatures for certain component within limits, the off-Sun angle of the –Z axis could not exceed 45°.

Figure 4 shows the Earth and Sun pointing constraints for TCM-1 for a representative Sun-spacecraft-Earth angle (about 90°) at TCM-1 and using (for illustrative purposes) the pre-launch values for the maximum off-Earth and off-Sun angles: ±80° and ±60°, respectively. The resulting allowable region for pointing the spacecraft –Z axis is the light purple region in Fig. 4. Note that this figure shows the projection of the Sun and Earth pointing constraints and allowable –Z-axis pointing regions on the Sun-spacecraft-Earth plane. The Sun and Earth pointing constraints are actually represented by cones in three dimensions. For purposes of performing propulsive maneuvers, the –Z axis of the spacecraft could be pointed anywhere within the light purple region.

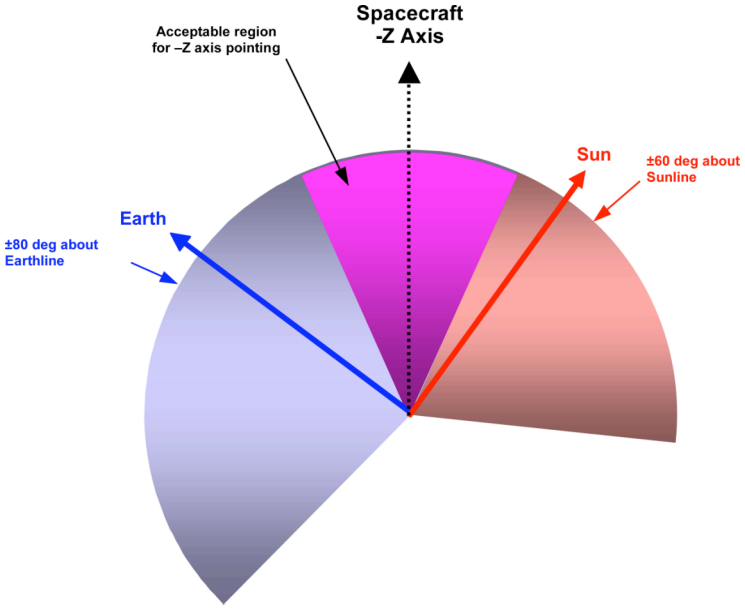

Figure 4: Propulsive maneuver pointing constraints.

Figure 5 shows various regions labeled with maneuver implementation modes permitted by pointing the spacecraft –Z axis in the allowable region identified on Fig. 4. TA indicates *turn and axial burn*, TL indicates *turn and lateral burn*, and TAL indicates *turn and vector mode burn*. A *vector mode (no turn)* maneuver implementation was always an option.

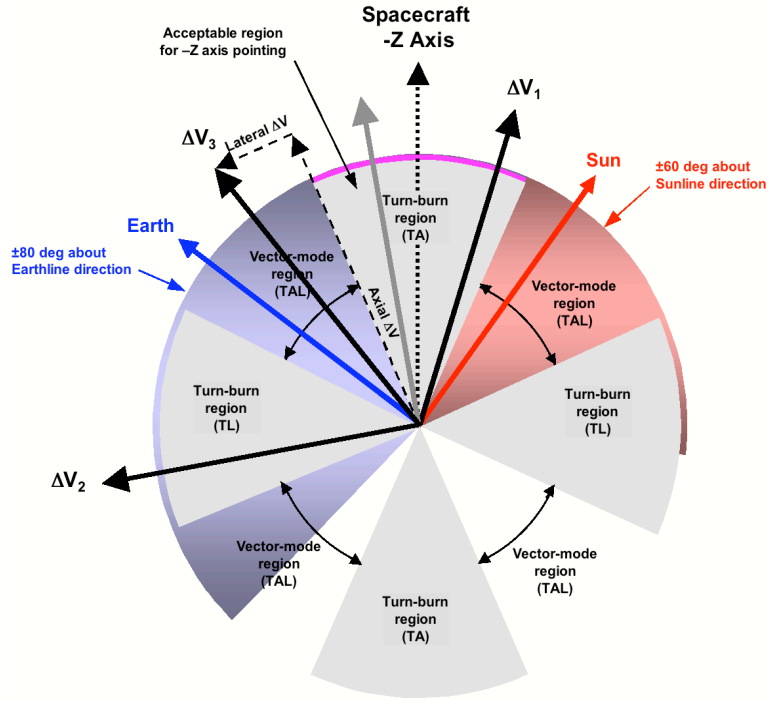

Figure 5: Propulsive maneuver modes.

Figure 5 also shows various possible desired ΔV vectors and allowable maneuver implementation modes for these ΔVs. For ΔV_1, the maneuver is most efficiently accomplished by a *turn and axial burn* in the –Z direction. For ΔV_2, the maneuver is most efficiently accomplished by a *turn and lateral burn*. For this case, the –Z axis would be pointed as indicated by the gray vector in the allowable –Z-axis pointing region. For ΔV_3, the maneuver is most efficiently accomplished by a *turn and vector mode burn*. For this case, the –Z axis would be pointed as indicated by the black dashed line labeled "Axial ΔV" on the border of the allowable –Z-axis pointing region. Recall that all TCMs except TCM-1 were accomplished with a *vector mode (no turn)* implementation. Thus, Fig. 5 illustrates possible maneuver implementation modes for TCM-1.

In order to make the TCM design process more efficient in terms of evaluating different maneuver implementation modes and constraints, special software (i.e., PORTIONM) was developed. The process of evaluating multiple maneuver implementation modes and PORTIONM are discussed in detail in [5].

G. Maneuver Execution Accuracy

The accuracy with which a given propulsive maneuver can be executed is a function of the propulsion system behavior and the attitude control system, which maintains the pointing of the spacecraft during thruster firings. Maneuver execution errors are described in terms of components that are proportional to the commanded ΔV magnitude and components that are independent of ΔV magnitude. The MER spacecraft design was required to satisfy the maneuver execution accuracy requirements listed in Table 7. These values were used during pre-launch analyses and during flight operations until late in the final approach phase for *Opportunity*, at which point the values listed in Table 4 were adopted, based on accumulated experience with spacecraft performance during preceding TCMs for both *Spirit* and *Opportunity*.

Table 7: Maneuver execution accuracy requirements.

Component	Error (3σ)
Proportional magnitude error	5%
Proportional pointing error, per axis	50 mrad (2.9°)
Fixed magnitude error	6 mm/s
Fixed pointing error, per axis	6 mm/s

H. TCM Targeting Process

For TCM design, the trajectory starting from the TCM and ending at a desired landing point on the surface of Mars was divided into two parts: the interplanetary (or exo-atmospheric) trajectory extending from the TCM to the atmospheric entry interface point (defined as Mars radius equal to 3522.2 km) and the atmospheric trajectory extending from the atmospheric entry interface point to landing. The TCM targets were the following parameters at the atmospheric entry interface point: entry time, inertial entry FPA, and B-plane angle. The inertial entry FPA was fixed at –11.5°. The entry time and B-plane angle both affected the latitude and longitude of the landing point. For any TCM design, the entry time and B-plane angle were determined to achieve the desired landing latitude and longitude. This was accomplished by the following process:

1. Select estimates for the entry time and B-plane angle (for example, from the previous TCM design).
2. Target the upcoming TCM to the fixed inertial entry FPA and the estimates of entry time and B-plane angle.
3. Generate a state vector at the atmospheric entry interface point.
4. Propagate the atmospheric trajectory from entry to the surface.
5. Determine the errors in landing latitude and longitude.
6. Adjust the entry time and B-plane angle. Go to Step 2.
7. Repeat the process until the errors in latitude and longitude are acceptably small.

This process used various computer programs from the navigation and mission design software sets. The primary programs were DPTRAJ/SEPV (TCM targeting) and AEPL (atmospheric propagation). Computer scripts were developed to automate this process in order to improve efficiency. Ultimately, the TCM design process became a highly automated procedure (see explanation in [5]).

I. Landing Dispersion Analysis (Landing Ellipses)

A key navigation capability was to calculate landing dispersions based on atmospheric entry delivery accuracies. These landing dispersions were referred to as landing ellipses, since an elliptical representation was used for displaying the landing dispersions at 99% probability. Landing dispersion analysis utilized an interface called the Entry State File (ESF). Whenever an interplanetary OD covariance study was performed (to estimate entry delivery accuracies) or a TCM design was completed, it was possible to generate an ESF containing 2001 dispersed entry states (the nominal entry state, corresponding to zero dispersion, plus 2000 dispersed states). These state vectors were specified at a fixed time 1 minute prior to the nominal epoch for the atmospheric entry interface point (Mars radius equal to 3522.2 km). The purpose for selecting a time 1 minute prior to the nominal entry time was to ensure that the actual entry times on the dispersed trajectories all occurred prior to the atmospheric entry interface point.

The ESF was utilized as input to perform a Monte Carlo trajectory analysis in which the nominal state vector and each of the 2000 dispersed entry state vectors were used as the initial state for propagating an atmospheric trajectory to the surface to determine a landing point. In addition to the dispersed initial states, uncertainties in the following models were also taken into account in the Monte Carlo analysis: atmospheric density, spacecraft and aerodynamics modeling, and wind variations. The resulting 2001 landing points were analyzed to generate an ellipse (i.e., landing ellipse) that represented the envelope of the landing dispersions at the 99% probability level. Two different software programs were used to perform the EDL Monte Carlo trajectory analyses: AEPL and POST. AEPL is a 3-DOF program developed at JPL, and POST is a 6-DOF program developed at the NASA Langley Research center (and run at JPL for use by MER navigation). POST was considered the "gold standard" and was used to verify AEPL results. Once the data for the landing ellipses had been generated, the ellipses were then visualized on a Mars surface map and further analyzed using a program called MarsLS. MarsLS is another software program developed specially for MER for landing dispersion analyses (and is intended to be used for the Genesis mission and for future Mars missions involving landers.)

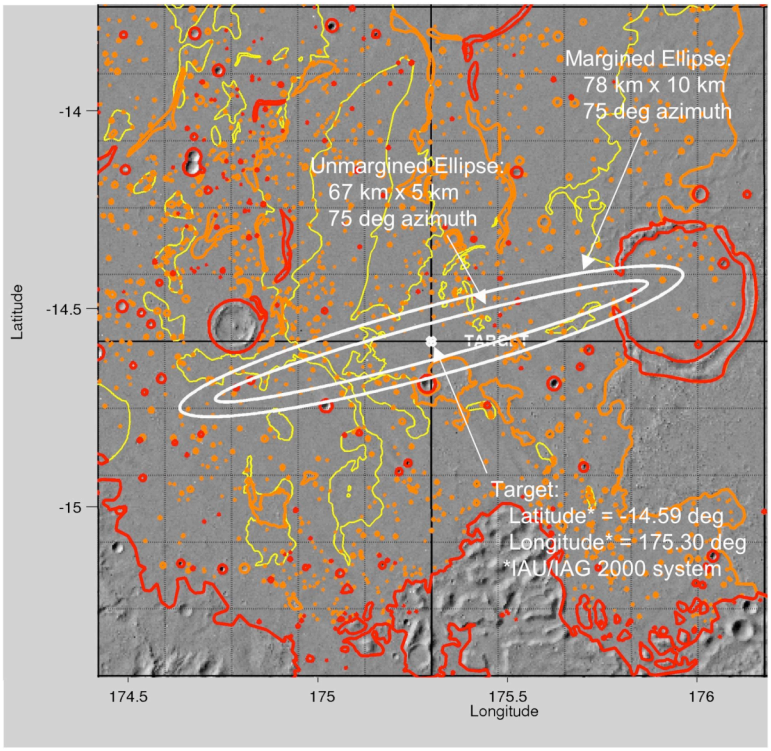

Figure 6: Gusev target landing ellipses.

The result of the Monte Carlo analysis described in the preceding paragraph was what was referred to as an unmargined ellipse. In order to account for unmodeled or unknown effects and to add a level of robustness to the landing ellipse for actual flight conditions that might fall outside the range of variations considered, margins were added in the downtrack and crosstrack directions to produce what were refereed to as margined ellipses. The effects addressed by these margins included errors in atmospheric density models, errors in wind models, navigation targeting margin, as well as other smaller effects (see [8]). The margin values for the individual contributors were root-sum-squared to obtain the final margins that were added to the unmargined ellipses to produce the margined ellipses: ±5.5 km in the downtrack direction and ±2.5 km in the crosstrack direction

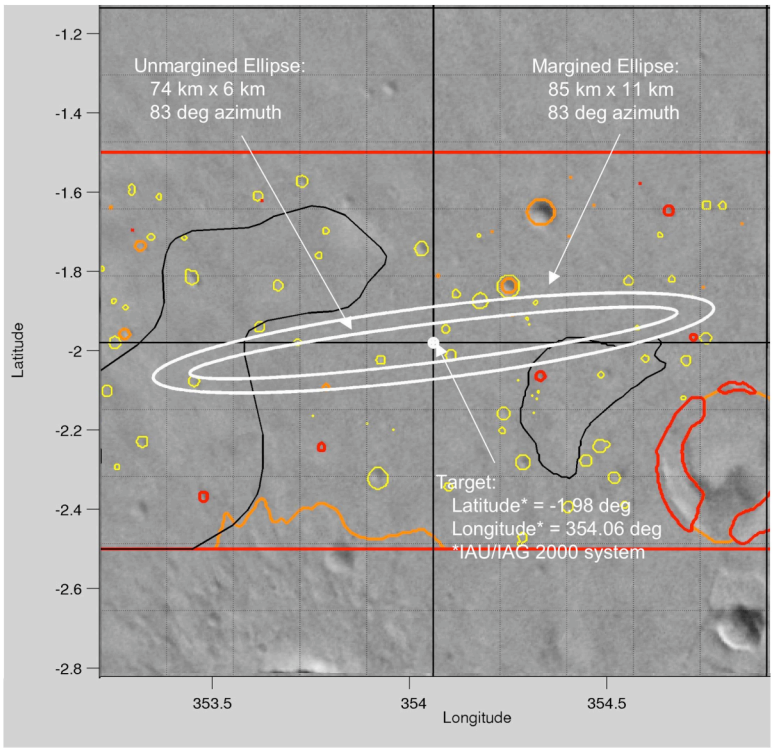

Figure 7: Meridiani target landing ellipses.

Landing ellipses generated by MarsLS were extensively used during

the MER development phase to support landing site selection and EDL hardware system design and trade studies. During flight operations, landing ellipses were used to evaluate probabilities of landing in hazardous areas, areas of Mars Orbiter camera (MOC) coverage, or areas of low nighttime temperatures. The probabilities of landing in hazardous areas of different types were combined with the probabilities of an in-spec (or successful) landing for that terrain type to produce a total probability of in-spec landing. The total probability of in-spec landing was one of the key factors in deciding whether a final approach TCM should be performed.

MarsLS plots of the target landing ellipses for *Spirit* (in Gusev Crater) and *Opportunity* (in Meridiani Planum) are shown in Figs. 6 and 7. These target ellipses correspond to TCM-5 entry FPA delivery errors of ±0.12° for *Spirit* and ±0.14° for *Opportunity*.

The MER landing dispersion analysis process and results are discussed in detail in [8].

VI. Interplanetary Cruise Navigation

A. Launch

1. Spirit

Spirit was launched on a Boeing Delta II 7925 launch vehicle from Cape Canaveral Air Force Station (CCAFS) Space Launch Complex 17A (SLC-17A) on June 10, 2003, at 17:58:47 UTC on the first of two instantaneous daily launch opportunities (93° launch azimuth). The *Spirit* launch and injection profile used a short-coast parking orbit. *Spirit* was targeted to arrive at Mars on January 4, 2004. The nominal 21-day launch period for *Spirit* extended from May 30, 2003, through June 19, 2003. Because of delays caused by spacecraft electrical problems (prior to spacecraft mating to launch vehicle) and weather problems, *Spirit* actually launched on the twelfth day of the nominal 21-day launch period.

The achieved injection conditions were as follows: $C_3 = 8.822\ km^2/s^2$, declination of the launch asymptote (DLA) = –2.32° (EME2000)[6], and right ascension of the launch asymptote (RLA) = 347.35° (EME2000). These injection conditions corresponded to the following error levels relative to the desired injection conditions and predicted injection statistics: –0.5 σ C_3 error, +1.0 σ DLA error, and +0.8 σ RLA error. These injection errors produced the following error levels in the Mars B-plane: +0.7 σ B•R error, +0.6 σ B•T error, and +0.7 σ time of closest approach (TCA) error. The injection from the Delta II launch vehicle into the *Spirit* interplanetary trajectory was extremely accurate (within 1σ of predicted dispersion at Mars).

2. Opportunity

Opportunity was launched on a Boeing Delta II 7925H launch vehicle from CCAFS SLC-17B on July 8, 2003, at 03:18:15 UTC on the second of two instantaneous daily launch opportunities (99° launch azimuth). The *Spirit* launch and injection profile used a long-coast parking orbit. *Opportunity* was targeted to arrive at Mars on January 25, 2004. The nominal 21-day launch period for *Opportunity* extended from June 25, 2003, through July 15, 2003. Because of delays caused by weather, cork insulation problems on the launch vehicle, problems with the battery in the launch vehicle flight termination system, and range violations, *Spirit* actually launched on the fourteenth day of the nominal 21-day launch period.

The achieved injection conditions were as follows: $C_3 = 14.322\ km^2/s^2$, DLA = –3.89° (EME2000), and RLA = 334.65° (EME2000). These injection conditions corresponded to the following error levels relative to the desired injection conditions and predicted injection statistics: 0.0 σ C_3 error, –0.8 σ DLA error, and +1.2 σ RLA error. These injection errors produced the following error levels in the Mars B-plane: –0.1 σ B•R error, –0.9 σ B•T error, and –0.1 σ TCA error. As for *Spirit*, the injection from the Delta II launch vehicle into the *Opportunity* interplanetary trajectory was also extremely accurate (within 1σ of predicted dispersion at Mars).

3. Injection Targeting: Central Landing Site

The injection targets for *Spirit* were consistent with a landing site that was referred to as the MER-A central landing site (CLS), approximately midway in longitude between the Gusev and Meridiani landing sites (see Fig. 8) and very close to the Isidis landing site. The reason is that, at the time the injection targets were generated, the landing site for *Spirit* had not been selected. At that time, the primary candidate landing sites for *Spirit* were Gusev and Isidis. However, the project also desired to have the option to target *Spirit* to Meridiani in the event that Meridiani was confirmed as the landing site for *Opportunity*, and the *Opportunity* launch failed (or did not occur). Thus, the CLS was used for the generation of injection targets in order to provide the option to target *Spirit* to any of the possible landing sites. The range of longitudes spanned by these landing sites was ±95° about the CLS.

[6] EME2000 coordinate system is defined as Earth Centered, Earth Mean Equator and Equinox of J2000.

An analogous situation existed for *Opportunity*. At the time the injection targets were generated, the landing site for *Opportunity* had not yet been officially confirmed; the candidate landing sites were Meridiani, Elysium, and Isidis. Thus, a CLS was also used for generating injection targets for *Opportunity*. The MER-B CLS (see Fig. 8) was approximately midway between Meridiani and Isidis, and Elysium was contained within the ±135° range of longitudes. The reason for not choosing the CLS to be on the opposite side of Mars, which would have resulted in a smaller ±45° range of longitudes, is that it was desired to have the *Opportunity* landing occur on the same calendar date regardless of which landing site was selected.

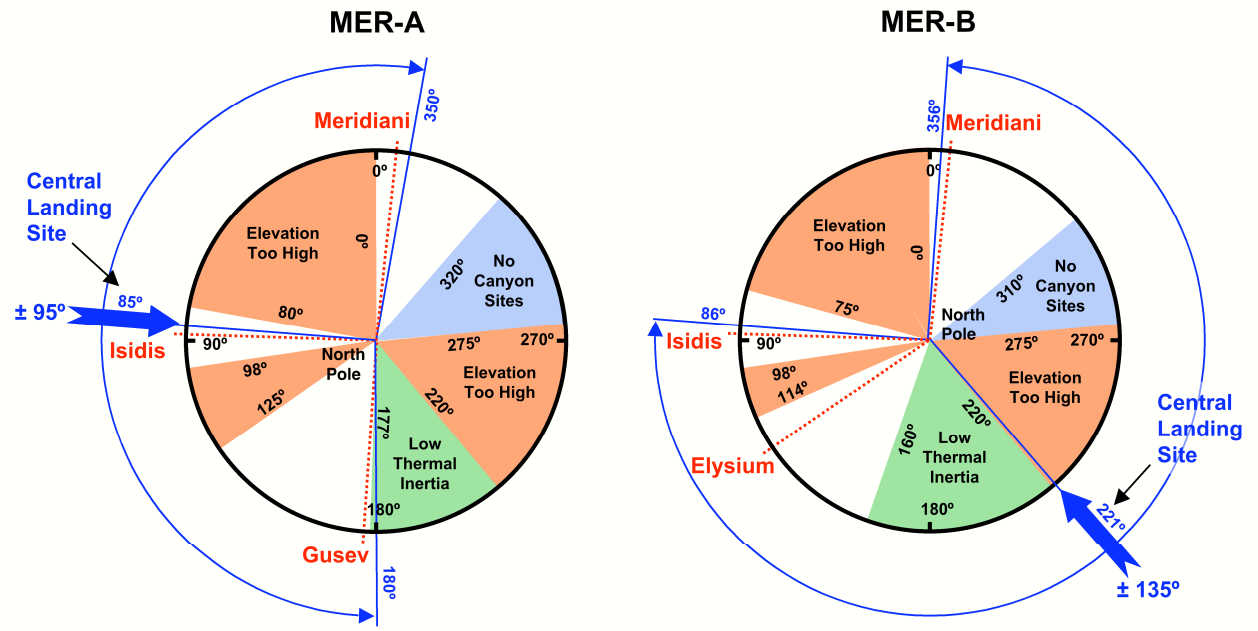

Figure 8: Central landing site targeting.

Subsequent to generation of the injection targets and prior to the launch of *Spirit*, changes had occurred to the candidate landing sites for both *Spirit* and *Opportunity*. Meridiani had been officially confirmed as the landing site for *Opportunity* (in April 2003), and the candidate landing sites for *Spirit* had been restricted to Gusev and Elysium. Originally, the latitude of the Elysium landing site had ruled it out as a candidate for *Spirit*, because of solar array power and mission efficiency considerations. However, Elysium was subsequently added as an additional candidate landing site for *Spirit*, in the event that Gusev was unable to be confirmed as a safe landing site. Elysium was identified as an additional safe, low-wind site along with Meridiani. Since from both a science and engineering safety perspective, Gusev was preferred over Isidis, the Isidis landing site was dropped from consideration. The project continued to maintain the option to target *Spirit* to Meridiani in the event that the *Opportunity* launch failed.

Thus the nominal plan for TCM targeting following launch was as follows: TCM-1 for *Spirit* would target to the MER-A CLS in order to remove injection errors and the trajectory bias introduced for planetary protection. If the launch of *Opportunity* failed, TCM-2 for *Spirit* would target to the Meridiani landing site. If the *Opportunity* launch was successful, TCM-2 for *Spirit* would target to a landing site midway between Gusev and Elysium, pending a final decision on the landing site. All TCMs for *Opportunity* would target to the Meridiani landing site.

B. Early Cruise: TCM-1

1. Spirit

TCM-A1 (TCM-1 for MER-A/*Spirit*) was performed 10 days after launch on June 20, 2003. TCM-A1 was executed as a vector-mode maneuver at the existing attitude (i.e., no spacecraft turns were involved) and consisted of a 28-minute continuous axial burn followed by 22 minutes of lateral burn pulses at an angle of 99° to the spacecraft –Z axis (negative spin axis) for a total velocity change of 16.5 m/s. The total magnitude of TCM-A1 was comparatively small (relative to predicted statistics), because of the accurate injection from the Delta launch vehicle. TCM-A1 served two primary purposes: to remove the bias in the spacecraft's trajectory introduced at launch to satisfy the planetary protection requirement for the Delta third stage (see Section IV.A) and to correct injection errors introduced by the launch vehicle. In addition, a lateral thruster calibration was included as part of TCM-A1. This permitted the use of larger lateral segments (i.e., more thruster pulses per segment prior to attitude and spin rate

corrections), which significantly reduced the duration of the maneuver. The landing site target for TCM-A1 was the MER-A CLS. This preserved the option to target *Spirit* to the Meridiani landing site in the event that the *Opportunity* launch failed or did not occur.

Figure 9 shows the B-plane for TCM-A1. This figure shows the Mars impact disk, the biased injection target and associated 3-sigma error ellipse, and the OD solution (OD03) used for the design of TCM-A1 and its associated 3-sigma uncertainties (not visible on the scale of the figure). The injection errors (magnitude of error in the B-plane and TCA error) are also labeled on this figure. Table 8 shows tabular data for TCM-A1: date and time, target parameters, achieved B-plane and entry conditions and associated 1-sigma uncertainties (as reconstructed following the maneuver), errors in the target parameters ("Achieved" minus "Target"), 1-sigma delivery uncertainties computed prior to the maneuver, and, finally, the errors in the target parameters expressed in units of delivery sigmas. The errors for TCM-A1 were all within one sigma with respect to predicted delivery uncertainties. Following TCM-A1, *Spirit* was not on an atmospheric entry trajectory. This result was not unexpected, given the large delivery uncertainties for TCM-A1. Table 9 shows the TCM-A1 implemented ΔV, maneuver magnitude and pointing errors for each maneuver component, and the total maneuver. The maneuver execution errors were all well within 3-sigma requirements for the flight system for maneuver performance.

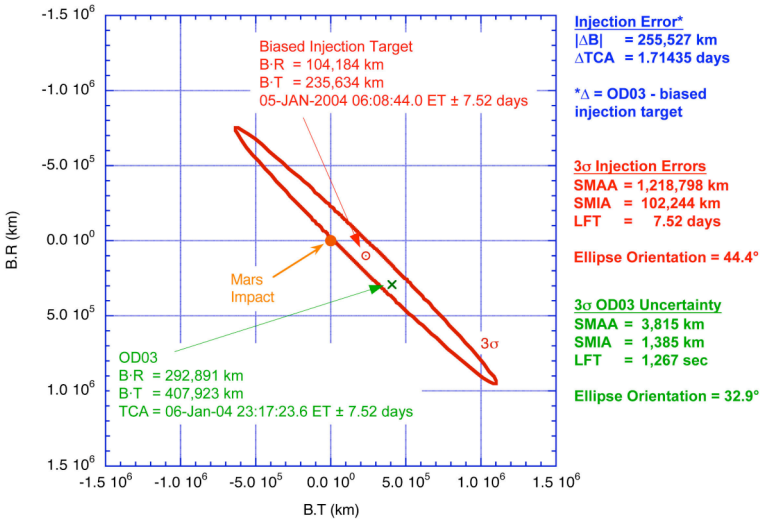

Figure 9: *Spirit* TCM-A1 B-plane.

2. Opportunity

TCM-B1 (TCM-1 for MER-B/*Opportunity*) was performed 10 days after launch on July 18, 2003. TCM-B1 consisted of a 49.3° turn to the required burn attitude followed by a 54-minute axial (+Z) burn for a total velocity change of 16.2 m/s. The total magnitude of TCM-B1 was small relative to predicted statistics, because of the accurate injection from the Delta launch vehicle. TCM-B1 served two primary purposes: to remove the bias in the spacecraft's trajectory introduced at launch to satisfy the planetary protection requirement for the Delta third stage (see Section IV.A) and to correct injection errors introduced by the launch vehicle. TCM-B1 was targeted to the Meridiani Planum landing site.

Figure 10 shows the B-plane for TCM-B1. This figure shows the Mars impact disk, the biased injection target and associated 3-sigma error ellipse, and the OD solution (OD03) used for the design of TCM-A1 and its associated 3-sigma uncertainties (not visible on the scale of the figure). The injection errors are also labeled on this figure. Table 10 shows tabular data for TCM-B1: date and time, target parameters, achieved B-plane and entry conditions and associated 1-sigma uncertainties, errors in the target parameters, 1-sigma delivery uncertainties computed prior to the maneuver, and, finally, the errors in the target parameters expressed in units of delivery sigmas. The B•R and B•T errors for TCM-B1 were less than one sigma with respect to predicted delivery uncertainties; the TCA error slightly exceeded the 1-sigma level. Following TCM-B1, *Opportunity* was not on an atmospheric entry trajectory. This

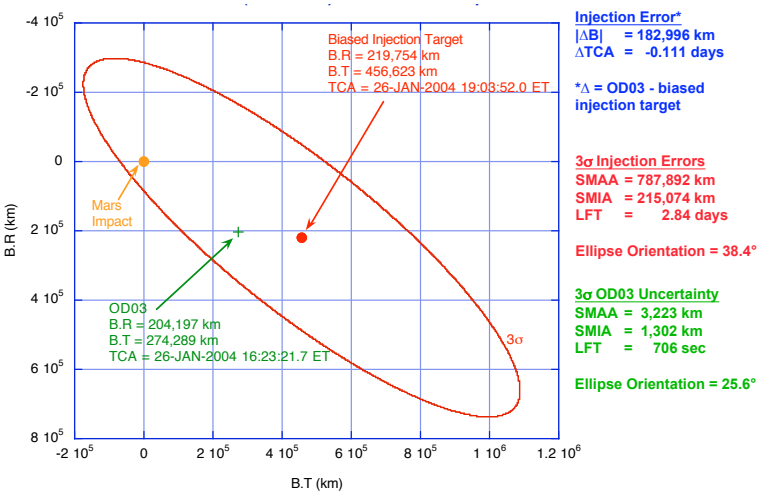

Figure 10: *Opportunity* TCM-B1 B-plane.

result was not unexpected, given the large delivery uncertainties for TCM-B1. Table 11 shows the TCM-B1 implemented ΔV, maneuver magnitude and pointing errors for each maneuver component, and the total maneuver. The maneuver execution errors were all well within 3-sigma requirements for the flight system for maneuver performance.

C. ACS/NAV Characterization

Following TCM-1 and prior to TCM-2, an ACS/NAV characterization activity was conducted for both the *Spirit* and *Opportunity* spacecraft. The objective of these activities was to characterize the magnitude of the ΔV caused by spacecraft turns. Because thrusters were fired as couples to accomplish a spacecraft turn, the nominal (i.e., expected) ΔV imparted to the spacecraft was zero. However, because of thruster misalignment and thrust imbalances, the actual ΔV resulting from a spacecraft turn was non-zero. It was important to characterize the magnitude of this residual ΔV, since assumptions had been made for this quantity in order to generate predicted atmospheric entry delivery accuracies and associated landing dispersions. Prior to performing the ACS/NAV characterization, the assumed value for residual ΔV was 3 mm/s (1σ) for all three components (line-of-sight, lateral, and normal).

The ACS/NAV characterization activities for *Spirit* and *Opportunity* were performed on July 21, 2003, and August 12, 2003. Each activity consisted of a large turn to an off-Earth attitude of about 45°, followed by eight 4.5° turns (about the turn size expected to occur during late cruise and final approach), and ending with a large turn back to the nominal cruise attitude. The eight intermediate turns were comprised of two identical sets of four turns: Turn #1 away from Earth, Turn #2 normal to Earth-line, Turn #3 normal to Earth-line (negative of Turn #2), and Turn #4 back toward Earth (negative of Turn #1). These four turns allowed a determination of three vector components of the residual ΔVs. Repeating the four-turn sequence provided additional data to reduce uncertainties in the estimates of residual ΔVs.

The results were very favorable. The residual ΔVs for the eight turns performed by *Spirit* averaged to 0.11 mm/s. For *Opportunity*, the corresponding value was slightly larger: 0.35 mm/s. In both cases, there was minimal variability in the residual ΔV over the eight turns. As compared to the pre-launch a priori assumption of 3 mm/s (1σ), the actual measured residual ΔVs were about an order of magnitude smaller. These results allowed the navigation team to reduce the a priori values for residual ΔV that were used both for performing covariance studies for atmospheric entry delivery accuracy and for cruise OD operations. The revised assumptions for delivery accuracy covariance studies were still kept somewhat conservative. The a priori value for residual ΔV (all three components) was reduced to 0.17 mm/s (1σ) for *Spirit* and 0.33 mm/s (1σ) for *Opportunity*. For cruise OD operations, smaller values were used. For *Spirit*, the a priori value for residual ΔV was set at 0.05 mm/s (1σ) for all three components. For *Opportunity*, the values used were 0.10 mm/s (1σ) for the line-of-sight component and 0.05 mm/s (1σ) for the other two components. The ACS/NAV characterization activity is discussed in detail in [3].

D. Mid Cruise: TCMs 2 and 3

1. Spirit

TCM-A2 was performed at launch plus 52 days on August 1, 2003 (42 days after TCM-A1). TCM-A2 was executed as a vector-mode maneuver at the existing attitude (no spacecraft turn) and consisted of a 9-minute continuous axial burn followed by 11 minutes of lateral burn pulses at 99° to the spacecraft –Z axis (negative spin axis) for a total velocity change of 6.0 m/s. TCM-A2 corrected the execution errors from TCM-A1 and retargeted *Spirit* from the MER-A CLS to the Gusev Crater landing site.

Prior to execution of TCM-A2, it was known that the *Opportunity* launch (and also TCM-B1) had been successful. Therefore, targeting *Spirit* to Meridiani was no longer necessary. However, at the time of TCM-A2, the decision between Gusev and Elysium for the landing site for *Spirit* still had not been made. Nevertheless, TCM-A2 was targeted to Gusev, because it was believed there was a high probability that Gusev would be selected as *Spirit*'s landing site, and it would be possible to retarget from Gusev to Elysium at TCM-A3, in the event that Elysium was selected. This strategy was possible because the *Spirit* injection errors were very small, and there was a resulting abundance of propellant margin. As it turned out, Gusev Crater was officially confirmed as the landing site for *Spirit* on September 26, 2003.

Figure 11 shows the B-plane for TCM-A2. Note that the impact disk for Mars is now clearly visible as is the error ellipse associated with OD06, which was used for the design of TCM-A2. Note also that the execution errors from TCM-A1 were quite small. The reason for this is that, to a certain extent, the errors from the axial and lateral components of TCM-A1 had canceled one another. The relatively large magnitude of TCM-A2 (6.0 m/s) was caused by the arrival time change required to retarget from the MER-A CLS to Gusev. Tables 8 and 9 contain data for the navigation performance and maneuver execution errors for TCM-A2. The B•R and B•T errors for TCM-A2 were less than one sigma with respect to predicted delivery uncertainties; the TCA error was at the 1.4σ level. Following TCM-A2, *Spirit* was not on an atmospheric entry trajectory (as was the case following TCM-A1). The primary reason is that TCM-A2 had a sizable deterministic component due to the landing site retargeting. Maneuver execution errors were well within flight system performance requirements.

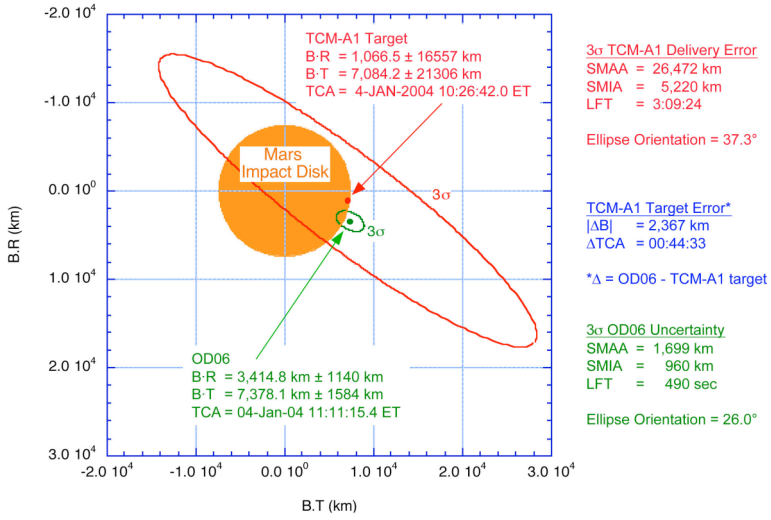

Figure 11: *Spirit* TCM-A2 B-plane.

TCM-A3 was performed on November 14, 2003, at E – 50 days. TCM-A3 was executed as a vector-mode maneuver at the existing attitude (no spacecraft turn) and consisted of a 2-minute continuous axial burn followed by 27 seconds of lateral burn pulses at 99° to the spacecraft –Z axis (negative spin axis) for a total velocity change of 0.6 m/s. TCM-A3 corrected the delivery errors from TCM-A2.

Figure 12 shows the B-plane for TCM-A3. As for TCM-A1, the execution errors from TCM-A2 were also quite small. Tables 8 and 9 contain data for the navigation performance and maneuver execution errors for TCM-A3. The B-plane and entry FPA errors for TCM-A3 were all less than one sigma with respect to predicted delivery uncertainties. Following TCM-A3, *Spirit* was, for the first time, on an atmospheric entry trajectory. Following TCM-A3, the predicted entry FPA error was –0.23°, and the predicted entry time error was +11 seconds. As for previous TCMs, the maneuver execution errors were well within flight system performance requirements.

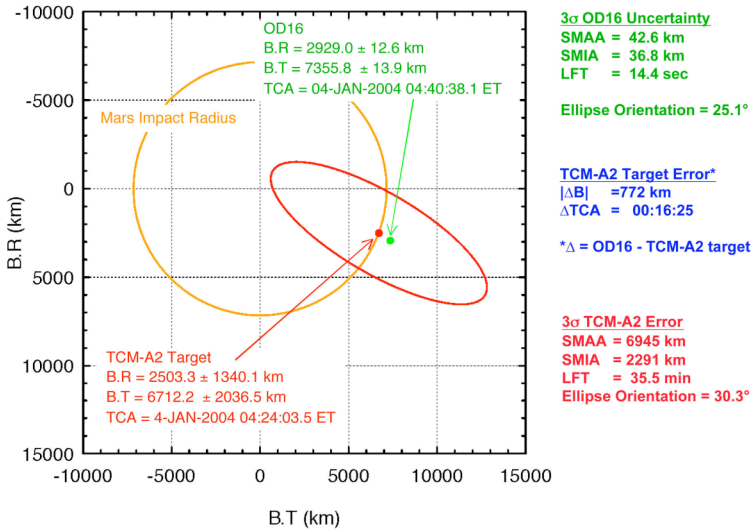

Figure 12: *Spirit* TCM-A3 B-plane.

2. Opportunity

TCM-B2 was performed at launch plus 62 days on September 8, 2003 (52 days after TCM-B1). TCM-B2 was executed as a vector-mode maneuver at the existing attitude (no spacecraft turn) and consisted of a 2-minute continuous axial burn followed by 16 seconds of lateral burn pulses at 99° to the spacecraft –Z axis (negative spin axis) for a total velocity change of 0.53 m/s. TCM-B2 corrected the execution errors from TCM-B1.

Figure 13 shows the B-plane for TCM-B2. Note that the execution errors from TCM-B1 were quite small (but larger than for TCM-A1). Tables 10 and 11 contain data for the navigation performance and maneuver execution errors for TCM-B2. The errors for TCM-B2 were less than one sigma with respect to predicted delivery uncertainties. Following TCM-B2, *Opportunity* was on an atmospheric entry trajectory with a predicted entry FPA

error of –2.2° and an entry time error of +49 seconds. The primary reason is that the magnitude of TCM-B2 was small (0.53 m/s), and the atmospheric entry delivery errors were dominated by maneuver execution errors (not OD errors), which are proportional to maneuver magnitude. The maneuver execution errors for TCM-B2 were well within flight system performance requirements.

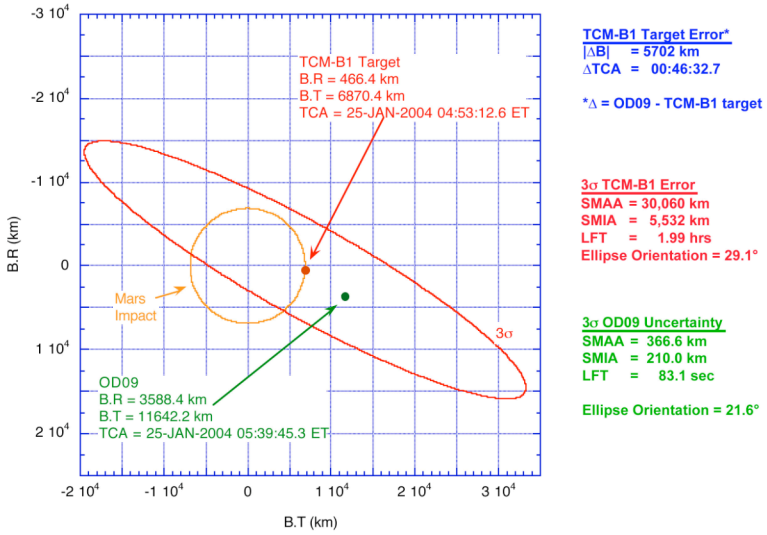

Figure 13: *Opportunity* TCM-B2 B-plane.

TCM-B3, which had been scheduled for November 21, 2003 (E – 65 days), was canceled. There were two primary reasons for this. First, because of excellent navigation and spacecraft performance at TCMs B1 and B2, the required velocity correction at TCM-B3 was very small (about 0.01 m/s). Cancellation of TCM-B3 would result in an increase to the magnitude of TCM-B4, but TCM-B4 would still be a very small maneuver (approximately 0.1 m/s). Second, as the start of development for TCM-B3 approached, the project recognized that the flight team was under a very heavy workload. This involved regular spacecraft operations, responses to disruptions in spacecraft activities caused by the effects of ongoing solar flares, and preparations for, and participation in, ongoing approach/EDL/surface Operations Readiness Tests (ORTs). For these reasons, TCM-B3 was canceled. Although the navigation team preferred executing TCM-B3 as originally planned to correct the delivery errors from TCM-B2, rather then waiting 57 days until the next maneuver opportunity at TCM-B4, the navigation team (with some reluctance) concurred with the decision to cancel TCM-B3.

Table 8: *Spirit* navigation performance summary.

TCM	Date/Time (UTC)	Parameter*	Units	Target	Achieved		Error	Delivery Uncertainty (1σ)	Error / Delivery Uncertainty (σ)
					Value	Uncertainty (1σ)			
A1	6/20/03 17:00	B•R	km	1,066.5	3,414.8	380	2,348.3	5,519	0.43
		B•T	km	7,084.2	7,378.1	528	293.9	7,102	0.04
		TCA	s	1/4/04 10:26:42.0	1/4/04 11:11:15.4	230	2,673.4	3,788	0.71
		FPA	deg	-11.5000	–	–	–	–	–
		θ	deg	8.5610	–	–	–	–	–
		T_E	s	1/4/04 10:23:21.9	–	–	–	–	–
A2	8/1/03 18:00	B•R	km	2,503.3	2,929.0	12.6	425.7	1,340	0.32
		B•T	km	6,712.2	7,355.8	13.9	643.6	2,037	0.32
		TCA	s	1/4/04 04:24:03.5	1/4/04 04:40:38.1	4.8	994.6	710	1.40
		FPA	deg	-11.5000	–	–	–	–	–
		θ	deg	20.4490	–	–	–	–	–
		T_E	s	1/4/04 04:20:43.5	–	–	–	–	–
A3	11/14/03 18:30	B•R	km	2,502.9	2,516.0	0.57	13.1	44.0	0.30
		B•T	km	6,711.6	6,700.3	0.35	-11.3	50.7	-0.22
		TCA	s	1/4/04 04:24:02.5	1/4/04 04:24:17.7	0.16	15.2	16.1	0.94
		FPA	deg	-11.5000	-11.7283	0.013	-0.2283	2.02	-0.11
		θ	deg	20.4480	20.5812	–	0.1332	–	–
		T_E	s	1/4/04 04:20:42.5	1/4/04 04:20:53.9	0.17	11.4	–	–
A4	12/27/03 02:00	B•R	km	2,504.99	2,504.94	0.48	-0.05	1.53	-0.03
		B•T	km	6,711.03	6,710.85	0.25	-0.18	1.50	-0.12
		TCA	s	1/4/04 04:24:15.7	1/4/04 04:24:15.8	0.011	0.1	0.53	0.21
		FPA	deg	-11.4871	-11.4943	0.0033	-0.0072	0.056	-0.13
		θ	deg	20.4655	20.4690	–	0.0035	–	–
		T_E	s	1/4/04 04:20:55.9	1/4/04 04:20:55.9	0.062	0.0	–	–
A5	1/2/04 02:00	Canceled							
A5X	1/3/04 02:00	Canceled							
A6	1/4/04 00:20	Canceled							

*B•R, B•T: Mars Equator of Date; TCA = closest approach time; FPA = inertial flight path angle; θ = B-plane angle; T_E = entry time.

Table 9: *Spirit* TCM execution errors.

TCM	Date/Time (UTC)	Implemented DV (m/s)[1]				Magnitude Error[2] (%)				Pointing Error[3] (mrad)			
		+Z	–Z	L	Total	+Z	–Z	L	Total	+Z	–Z	L	Total
A1	6/20/03 17:00	9.103		12.376	16.460	-3.9%		+1.0%	-0.7%	11.6		0.1	22.5
A2	8/1/03 18:00	2.317		5.207	6.008	-1.4%		-2.6%	-2.4%	0.3		2.5	2.3
A3	11/14/03 18:30	0.513		0.200	0.577	-1.6%		-0.4%	-1.7%	12.9		3.8	9.9
A4	12/27/03 02:00			0.025	0.025			-1.4%	-1.4%			5.5	5.5
A5	1/2/04 02:00	Canceled											
A5X	1/3/04 02:00	Canceled											
A6	1/4/04 00:20	Canceled											

[1]+Z = along spacecraft +Z axis; –Z = along spacecraft –Z axis; L = lateral ΔV component.
[2]Requirement = 5% (3σ). [3]Requirement = 50 mrad (3σ).

Table 10: *Opportunity* navigation performance summary.

TCM	Date/Time (UTC)	Parameter*	Units	Target (Times are ET)	Achieved		Error	Delivery Uncertainty (1σ)	Error / Delivery Uncertainty (σ)
					Value	Uncertainty (1σ)			
B1	7/18/03 19:30	B•R	km	466.4	3,588.4	79	3,122.0	5,112	0.61
		B•T	km	6,870.4	11,642.2	116	4,771.8	8,799	0.54
		TCA	s	1/25/04 04:53:12.6	1/25/04 05:39:45.3	36	2,792.7	2,388	1.17
		FPA	deg	-11.5000	–	–	–	–	–
		θ	deg	3.8850	–	–	–	–	–
		T_E	s	1/25/04 04:49:57.9	–	–	–	–	–
B2	9/8/03 16:00	B•R	km	466.4	419.5	0.51	-46.9	148	-0.32
		B•T	km	6,870.2	6,814.5	0.29	-55.7	222	-0.25
		TCA	s	1/25/04 04:53:11.9	1/25/04 04:52:58.1	0.15	-13.8	36.2	-0.38
		FPA	deg	-11.5000	-13.6791	0.0095	-2.1791	–	–
		θ	deg	3.8850	3.5224	–	-0.3626	–	–
		T_E	s	1/25/04 04:49:57.2	1/25/04 04:49:08.4	0.18	-48.8	–	–
B3	11/21/03 18:30	Canceled							
B4	1/17/04 02:00	B•R	km	465.81	466.88	0.44	1.07	2.49	0.43
		B•T	km	6,870.18	6,870.86	0.20	0.68	2.38	0.29
		TCA	s	1/25/04 04:52:59.1	1/25/04 04:53:00.1	0.015	1.0	0.82	1.23
		FPA	deg	-11.5000	-11.4699	0.0070	0.0301	0.096	0.31
		θ	deg	3.8796	3.8873	–	0.0077	–	–
		T_E	s	1/25/04 04:49:44.4	1/25/04 04:49:45.9	0.13	1.5	–	–
B5	1/23/04 02:00	Canceled							
B5X	1/24/04 02:00	Canceled							
B6	1/25/04 00:50	Canceled							

*B•R, B•T: Mars Equator of Date; TCA = closest approach time; FPA = inertial flight path angle; θ = B-plane angle; T_E = entry time.

Table 11: *Opportunity* TCM execution errors.

TCM	Date/Time (UTC)	Implemented DV (m/s)[1]				Magnitude Error[2] (%)				Pointing Error[3] (mrad)			
		+Z	–Z	L	Total	+Z	–Z	L	Total	+Z	–Z	L	Total
B1	7/18/03 19:30	16.172			16.172	-1.4%			-1.4%	3.0			3.0
B2	9/8/03 16:00	0.496		0.136	0.534	+1.8%		-0.6%	+1.1%	7.2		11.4	11.1
B3	11/21/03 18:30	Canceled											
B4	1/17/04 02:00		0.083	0.081	0.107		+2.9%	-1.9%	+0.6%		8.7	7.7	34.0
B5	1/23/04 02:00	Canceled											
B5X	1/24/04 02:00	Canceled											
B6	1/25/04 00:50	Canceled											

[1]+Z = along spacecraft +Z axis; –Z = along spacecraft –Z axis; L = lateral ΔV component.
[2]Requirement = 5% (3σ). [3]Requirement = 50 mrad (3σ).

E. Final Approach: TCMs 4, 5, and 6

The focus for the final approach phase TCMs was primarily directed at monitoring and correcting errors to atmospheric entry FPA and landing location (latitude and longitude) and ensuring a safe landing. Miss distance from the desired landing point, the probability of an in-spec (i.e., safe) landing (described in Section V.I. and in [8]), and numerous other factors were used extensively in evaluating the requirement to perform a TCM. Notable among the other factors were stability and consistency of OD solutions and an evaluation by the science team of the predicted landing point in terms of environmental safety (e.g., terrain and wind characteristics) and relative science return (i.e., desirability or undesirability of the landing location).

1. *Spirit*

TCM-A4 was performed on December 27, 2003, at E – 8 days. This TCM corrected the delivery errors from TCM-A3. Following TCM-A3, the entry FPA error was –0.23°, and the miss distance from the desired landing point was 54 km. TCM-A4 was executed as a vector-mode maneuver at the existing attitude (no spacecraft turn) with only a lateral component consisting of a single 3.4-s lateral pulse. The total velocity change for TCM-A4 was 0.03 m/s.

If TCM-A4 had been implemented with both axial and lateral components, the path of the maneuver on the surface (i.e., the locus of instantaneous impact points during the maneuver) would have been highly undesirable. Because of the high correlation between errors in entry FPA and downtrack position on the surface (mostly longitude), in order to correct all three target variables (entry FPA and latitude and longitude of the landing point), the miss distance (primarily in the downtrack direction) following the first maneuver component would have increased to either about 170 km (axial component executed first) or about 115 km (lateral component executed first). The second maneuver component would reverse the large movement in the downtrack direction and return the landing point to the target. However, implementing TCM-A4 as a lateral-only maneuver provided a way to exactly correct the errors in latitude and longitude, while incurring a very small (and entirely acceptable) error in entry FPA. In the case of TCM-A4, the error in entry FPA caused by the lateral-only maneuver implementation was only +0.013°. Thus, the target entry FPA for TCM-A4 was –11.487°. The special maneuver implementation strategies to deal with eliminating undesirable paths of the landing point during the maneuver are explained in [5].

Figure 14 shows the B-plane for TCM-A4, and Fig. 15 shows the path of the maneuver on the surface. Tables 8 and 9 contain data for the navigation performance and maneuver execution errors for TCM-A4. The quantities labeled as "Achieved" correspond to the final OD update prior to atmospheric entry. The errors for TCM-A4 were all much less than one sigma with respect to predicted delivery uncertainties. The maneuver execution errors for TCM-A4 were also very small. Following TCM-A4, OD solutions indicated that the maneuver performance had been excellent. The landing point was estimated to be only about 2 km from the target.

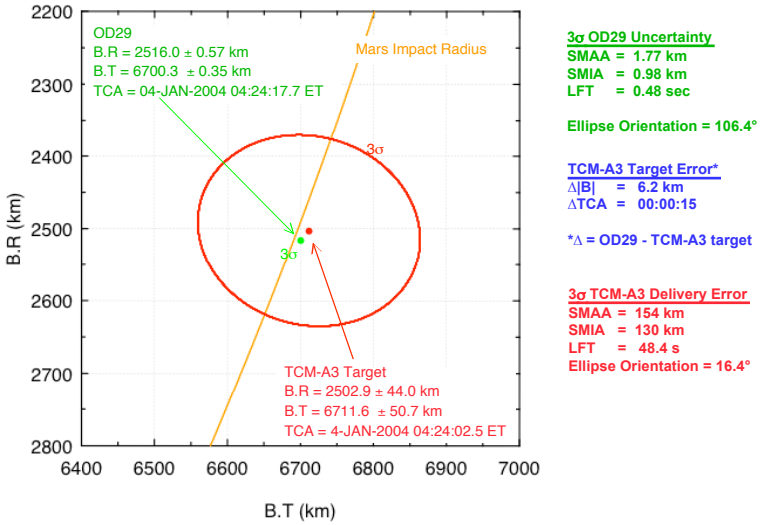

Figure 14: *Spirit* TCM-A4 B-plane.

TCM-A5 was scheduled for January 2, 2004, at E – 2 days. At the decision point for TCM-A5, the latest OD solution (OD33) indicated that the predicted landing point was only 2.3 km from the target in the uptrack direction. This is shown in Fig. 16, which illustrates the predicted landing point and associated unmargined and margined landing, ellipses based on OD33. Results for OD33 (including predicted entry conditions and miss distance on the surface) are shown in Table 12. The error in entry FPA of +0.001° was inconsequential. The entry FPA uncertainty was estimated to be ±0.028° (3σ). The size of the unmargined landing ellipse was 63 km x 3 km.[7] (Given the extremely small entry FPA uncertainty, the size of the landing ellipse was no

[7] During final approach for Spirit, atmospheric density models for the Gusev landing site were being evaluated on a regular basis. As of OD33, a new baseline density model was adopted. This change caused the downtrack dimension of the landing ellipses to increase by about 50% as compared to prior analyses (including those done only a few days earlier). The effects of atmospheric density models on landing dispersions are discussed in [8].

longer dominated by navigation errors at atmospheric entry, but rather by atmosphere and spacecraft aerodynamics modeling uncertainties.) Based on landing dispersion analyses, the probability of an in-spec landing was extremely high, OD solutions leading up to the TCM-A5 decision point had been consistent and stable, and a science evaluation of the predicted landing point was favorable. Consequently, TCM-A5 was canceled. Cancellation of TCM-A5 led automatically to cancellation of TCM-A5X as well. TCM-A5X was an emergency backup maneuver that would have been performed if TCM-A5 had failed.

The situation for TCM-A6 was similar to that for TCM-A5. TCM-A6 was scheduled for E – 4 hours as a final opportunity to correct the trajectory. However, the OD solutions had remained remarkably stable since the cancellation of TCM-A5. The results for OD38 (the basis for the TCM-A6 decision) are shown in Table 12. The changes from OD33 are negligible. The predicted miss distance from the target landing point for OD38 was 2.1 km, and the entry FPA error was a still inconsequential –0.002°. The entry FPA uncertainty had decreased slightly to ±0.024° (3σ). The size of the unmargined landing ellipse remained at 63 km x 3 km (dominated by atmosphere and spacecraft aerodynamics modeling uncertainties). Results from landing dispersion analyses (probability of in-spec landing and science evaluations) were favorable for the predicted landing point. Thus, TCM-A6 was also canceled.

The final OD update (OD46) prior to atmospheric entry is shown in Table 12. OD46 was based on a navigation tracking data cutoff at the termination of two-way tracking at E – 105 minutes (coincident with the switch from the cruise stage MGA to the LGA). The estimated atmospheric entry quantities had hardly changed from OD38. The predicted miss distance from the target landing point was 3.3 km. The entry FPA error was –0.007° (still negligible). By this time, the entry FPA uncertainty had decreased to only ±0.0099° (3σ). The size of the unmargined landing ellipse remained at 63 km x 3 km (dominated by atmosphere and spacecraft aerodynamics modeling uncertainties).

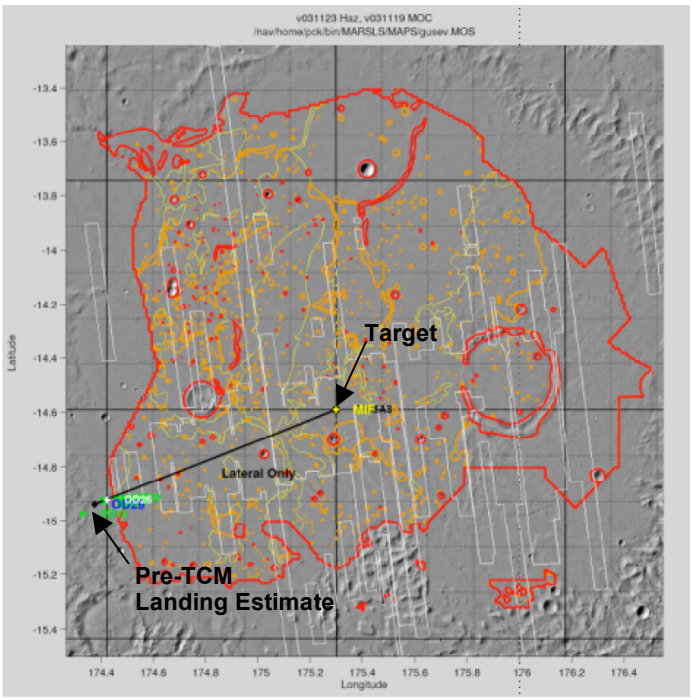

Figure 15: *Spirit* TCM-A4 path on surface.

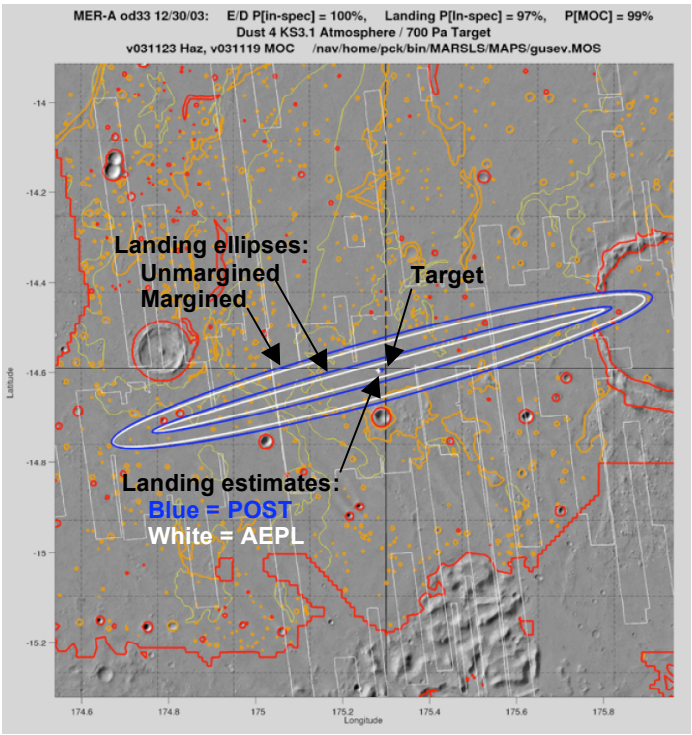

Figure 16: *Spirit* OD33 landing point and dispersions.

Table 12: *Spirit* orbit determination results and landing point miss distances following TCM-A4.

OD #	Data Cutoff (UTC)	Parameter*	Units	Target	OD Solution		Error
					Value	Uncertainty (1σ)	
33 (TCM-A5 Design)	1/2/04 02:00	B•R	km	2,504.99	2,504.91	0.56	-0.08
		B•T	km	6,711.03	6,711.08	0.33	0.05
		TCA	s	1/4/04 04:24:15.7	1/4/04 04:24:15.8	0.12	0.1
		FPA	deg	-11.4871	-11.4861	0.0093	0.0010
		θ	deg	20.4655	20.4681	–	0.0026
		T_E	s	1/4/04 04:20:55.9	1/4/04 04:20:56.0	0.11	0.1
		Surface Miss	km				2.3
38 (TCM-A6 Design)	1/4/04 00:20	B•R	km	Same as above.	2,505.12	0.51	0.13
		B•T	km		6,710.91	0.26	-0.12
		TCA	s		1/4/04 04:24:15.8	0.11	0.1
		FPA	deg		-11.4895	0.0079	-0.0024
		θ	deg		20.4701	–	0.0046
		T_E	s		1/4/04 04:20:55.9	0.085	0.0
		Surface Miss	km				2.1
46 (Final Pre-entry Update)	1/4/04 02:30	B•R	km	Same as above.	2,504.94	0.48	-0.05
		B•T	km		6,710.85	0.25	-0.18
		TCA	s		1/4/04 04:24:15.8	0.011	0.1
		FPA	deg		-11.4943	0.0033	-0.0072
		θ	deg		20.4690	–	0.0035
		T_E	s		1/4/04 04:20:55.9	0.062	0.0
		Surface Miss	km				3.3

*B•R, B•T: Mars Equator of Date; TCA = closest approach time; FPA = inertial flight path angle; θ = B-plane angle; T_E = entry time.

2. Opportunity

TCM-B4 was performed on January 17, 2004, at E – 8 days. This TCM corrected the delivery errors from TCM-B2, since TCM-B3 had been canceled. Following TCM-B2, the entry FPA error was –2.2°, and the miss distance from the desired landing point was 384 km. The large entry FPA error and miss distance (as compared to the equivalent errors for *Spirit* at TCM-A4) were directly a consequence of not performing TCM-B3. The execution errors from TCM-B2 had a significantly longer time to accumulate. TCM-B4 was executed as a vector-mode maneuver at the existing attitude (no spacecraft turn) and consisted of a 20-second continuous axial burn followed by 10 seconds of lateral burn pulses at 98° to the spacecraft –Z axis (negative spin axis) for a total velocity change of 0.11 m/s.

Since the errors being corrected by TCM-B4 were relatively large, there was no issue with respect to the path of the maneuver on the surface. Both axial and lateral components of TCM-B4 moved the landing point closer to the target. The axial component reduced the miss distance from 384 km to 77 km, and the lateral component corrected the remaining error. Implementing TCM-B4 with both axial and lateral components also meant that a full correction of the entry FPA (to the desired value of –11.5°) was part of the maneuver design.

Figure 17 shows the B-plane for TCM-B4, and Fig. 18 shows the path of the maneuver on the surface. Tables 10 and 11 contain data for the navigation performance and maneuver execution errors for TCM-B4. The quantities labeled as "Achieved" correspond to the final OD update prior to atmospheric entry. The errors for TCM-B4 were, with the exception of TCA, less than one sigma with respect to predicted delivery uncertainties; the TCA error was slightly greater than one sigma. The maneuver execution magnitude error for TCM-B4 was very small, but the maneuver execution pointing error (34.0 mrad) was the largest seen for any TCM for either *Spirit* or *Opportunity*. Because the magnitude of TCM-B4 was much larger than it would have been if TCM-B3 had not been canceled, the post-maneuver errors (e.g., entry FPA and miss distance on the surface) were corresponding larger. Following TCM-B4, OD solutions showed that the landing point was estimated to be about 10 km from the target (as compared to about 2 km for *Spirit* following TCM-A4).

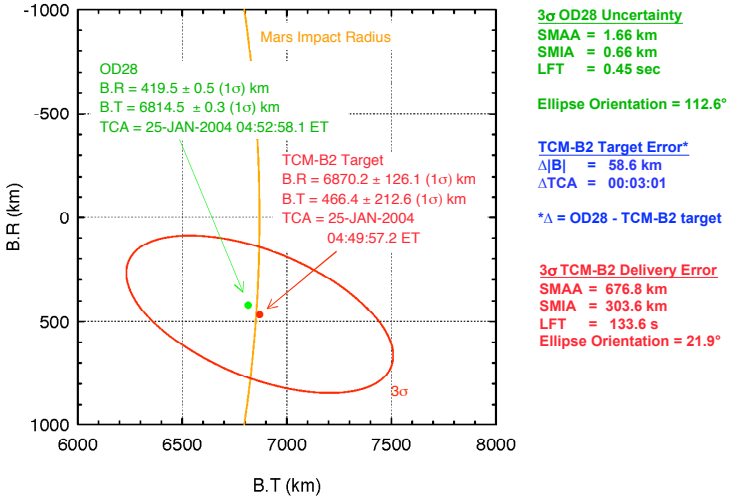

Figure 17: *Opportunity* TCM-B4 B-plane.

TCM-B5 was scheduled for January 22, 2004, at E – 2 days. At the decision point for TCM-B5, the latest OD solution (OD34) indicated that the predicted landing point was 9.6 km from the target in the downtrack direction. This is shown in Fig. 19, which illustrates the predicted landing point and associated unmargined and margined landing ellipses based on OD34. Results for OD34 (including predicted entry conditions and miss distance on the surface) are shown in Table 13. The error in entry FPA (+0.035°) was not an issue. The entry FPA uncertainty was estimated to be ±0.034° (3σ). The size of the unmargined landing ellipse was 61 km x 4 km. (As for *Spirit*, the small entry FPA uncertainty at this point meant that the size of the landing ellipse was dominated by atmosphere and spacecraft aerodynamics modeling uncertainties.) Based on landing dispersion analyses, the probability of an in-spec landing was extremely high, and the OD solutions leading up to the TCM-B5 decision point had been consistent and stable. A science evaluation of the predicted landing point resulted in a recommendation by the science team to perform TCM-B5 to move the landing point to a location that had more scientifically interesting terrain. At this time, however, *Spirit* was experiencing a problem with its flash memory. Consequently, the project decided to cancel TCM-B5 in order to devote flight team resources to addressing the *Spirit* problem. Cancellation of TCM-B5 led automatically to cancellation of TCM-B5X as well. TCM-B5X was an emergency backup maneuver that would have been performed if TCM-B5 had failed.

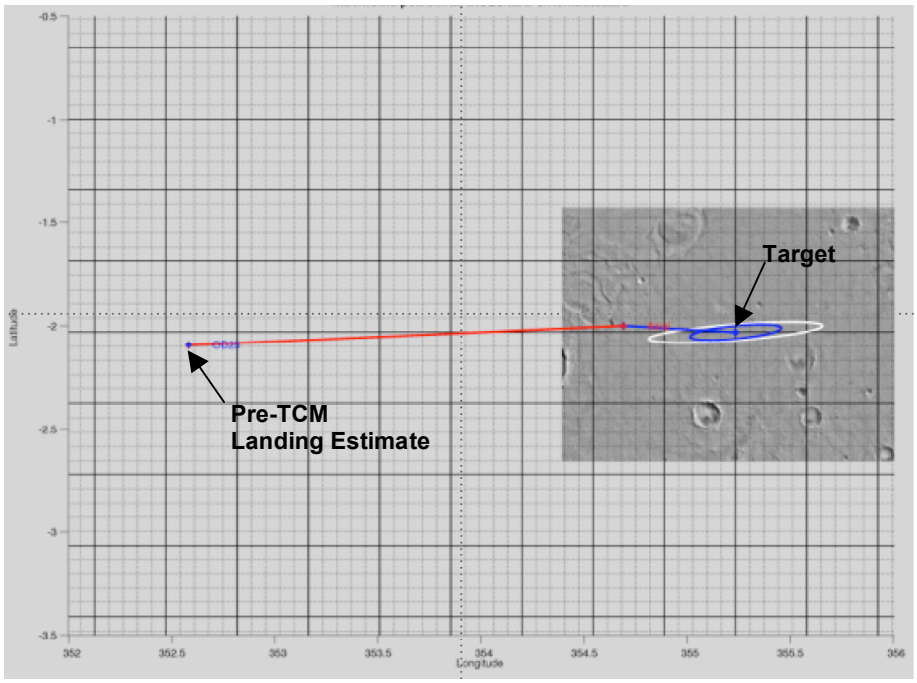

Figure 18: ***Opportunity*** **TCM-B4 path on surface.**

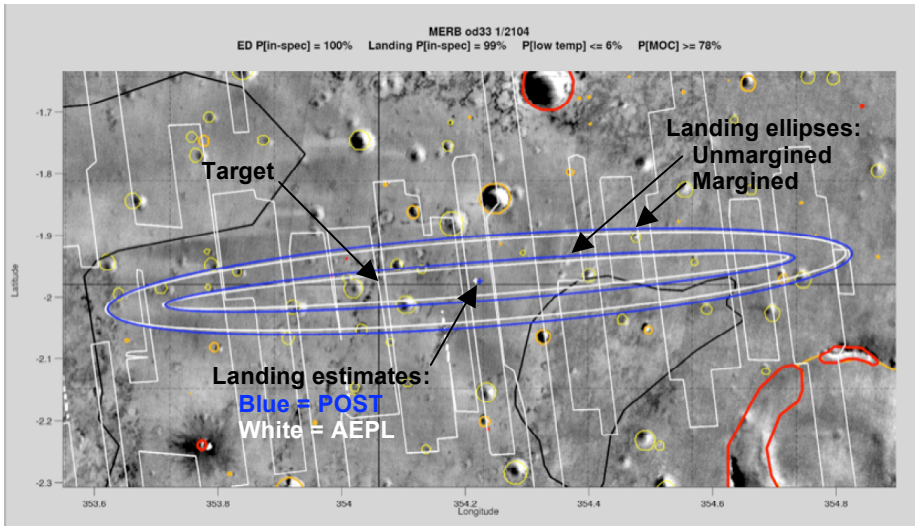

Figure 19: ***Opportunity*** **OD33 (Same as OD34) landing point and dispersions.**

The situation for TCM-B6 was similar to that for TCM-B5. TCM-B6 was scheduled for E – 4 hours as a final opportunity to correct the trajectory. However, the OD solutions had remained remarkably stable since the cancellation of TCM-B5. The results for OD38 (the basis for the TCM-B6 decision) are shown in Table 13. The changes from OD34 are inconsequential. The predicted miss distance from the target landing point for OD38 was 10.6 km, and the entry FPA error was essentially unchanged at +0.034°. The entry FPA uncertainty increased slightly to ±0.040° (3σ). The size of the unmargined landing ellipse remained at 61 km x 4 km (dominated by atmosphere and spacecraft aerodynamics modeling uncertainties). Results from landing dispersion analyses

Table 13: *Opportunity* orbit determination results and landing point miss distances following TCM-B4.

OD #	Data Cutoff (UTC)	Parameter*	Units	Target (Times are ET)	OD Solution		Error
					Value	Uncertainty (1σ)	
34 (TCM-A5 Design)	1/23/04 02:00	B•R	km	465.81	466.74	0.76	0.93
		B•T	km	6,870.18	6,870.98	0.32	0.80
		TCA	s	1/25/04 04:52:59.1	1/25/04 04:53:00.1	0.18	1.0
		FPA	deg	-11.5000	-11.4653	0.0115	0.0347
		θ	deg	3.8796	3.8861	–	0.0065
		T_E	s	1/25/04 04:49:44.4	1/25/04 04:49:46.0	0.24	1.6
		Surface Miss	km				9.6
38 (TCM-A6 Design)	1/25/04 00:50	B•R	km	Same as above.	466.52	0.84	0.71
		B•T	km		6,870.98	0.38	0.80
		TCA	s		1/25/04 04:53:00.2	0.047	1.1
		FPA	deg		-11.4659	0.0132	0.0341
		θ	deg		3.8842	–	0.0046
		T_E	s		1/25/04 04:49:46.0	0.26	1.6
		Surface Miss	km				10.6
41 (Final Pre-entry Update)	1/25/04 03:00	B•R	km	Same as above.	466.88	0.44	1.07
		B•T	km		6,870.86	0.20	0.68
		TCA	s		1/25/04 04:53:00.1	0.015	1.0
		FPA	deg		-11.4699	0.0070	0.0301
		θ	deg		3.8873	–	0.0077
		T_E	s		1/25/04 04:49:45.9	0.13	1.5
		Surface Miss	km				9.7

*B•R, B•T: Mars Equator of Date; TCA = closest approach time; FPA = inertial flight path angle; θ = B-plane angle; T_E = entry time.

(probability of in-spec landing and science evaluations) were favorable for the predicted landing point. Thus, TCM-A6 was also canceled.

The final OD update (OD41) prior to atmospheric entry is shown in Table 13. OD41 was based on a navigation tracking data cutoff at the termination of two-way tracking at E – 105 minutes (coincident with the switch from the cruise stage MGA to the LGA). The estimated atmospheric entry quantities had hardly changed from OD38, and the predicted miss distance from the target landing point was 9.7 km. By this time, the entry FPA error was +0.030° (slightly reduced). The entry FPA uncertainty had decreased to ±0.021° (3σ). The size of the unmargined landing ellipse remained at 61 km x 4 km (dominated by atmosphere and spacecraft aerodynamics modeling uncertainties).

F. Final Approach: EDL Parameter Updates

During final approach for both *Spirit* and *Opportunity*, three opportunities were provided for updating parameters in the EDL behavior that consisted of the sequence of spacecraft commands for EDL coded into flight software. The EDL sequence was executed autonomously by the spacecraft to perform the various EDL events in order to ensure a safe landing. These events included telecom system reconfiguration, spacecraft turn to entry attitude, venting of the heat rejection system (HRS), cruise stage separation, parachute deployment, airbag inflation, RAD rocket firing, etc.

The parameters in the EDL sequence that could be updated were specified in two files generated by the navigation team: the Entry Target and Landing File (ETLF) and the Parachute Deploy Parameter File (PDPF). The parameters in the ETLF included (among others) entry time, spacecraft attitude at entry, landing time, latitude and longitude of the landing point, local vertical and north vectors at landing, and sun vector at landing. The parameters in the PDPF included (among others) time from entry for the backup parachute deploy timer, backup parachute deploy timer uncertainties, time correction polynomial coefficients for the parachute deeply algorithm, and other parachute deploy algorithm architectural parameters.

The schedule for the three planned EDL parameter updates for both *Spirit* and *Opportunity* was as follows:

EDL Parameter Update #1	E – 6 days (TCM-4 plus 2 days)
EDL Parameter Update #2	E – 28 hours (TCM-5 plus ~1 day)
EDL Parameter Update #3	E – 2.7 hours (TCM-6 plus 75 minutes)

The outcomes of the EDL parameter updates for *Spirit* and *Opportunity* are briefly described in the remainder of this section.

1. *Spirit*

EDL Parameter Update #1 (After TCM-A4)

EDL parameter update #1 provided an opportunity to update the EDL sequence parameters following execution of TCM-A4. The analysis for this update was based on OD solution OD31 (delivered after TCM-A4 on December 28, 2003), a targeted parachute deploy dynamic pressure of 700 Pa, and atmosphere model "Ksv2.4.1". The results of the analysis determined that an update was required, because there had been a delay in the atmospheric entry time of 13 seconds caused by implementation of TCM-A4 as a lateral-only maneuver. The updated EDL parameters were uplinked to the spacecraft on December 28, 2003.

EDL Parameter Update #2 (After TCM-A5)

EDL parameter update #2 provided an opportunity to update the EDL sequence parameters following execution of TCM-A5. Even though TCM-A5 was not performed, an EDL parameter update analysis was carried out. This analysis was based on OD31 (delivered on January 2, 2004), a targeted parachute deploy dynamic pressure of 725 Pa, and atmosphere model "Ksv3.1 Dust 4". The results of the analysis determined that an update was required, because the targeted dynamic pressure for parachute deploy had increased, and the atmosphere dust model had changed. The updated EDL parameters were uplinked to the spacecraft on January 2, 2004.

EDL Parameter Update #3 (With TCM-A6 Design)

EDL parameter update #3 provided an opportunity to update the EDL sequence parameters in the event that there was a late change in the trajectory (i.e., atmospheric entry conditions) whether or not TCM-A6 was executed. As has been noted previously, TCM-A6 was not performed. The EDL parameter update analysis was based on OD44 (delivered on January 3, 2004), a targeted parachute deploy dynamic pressure of 725 Pa, and atmosphere model "Ksv3.1 Dust 4". The analysis determined that no update to the EDL parameters was required. There had been no changes to either the targeted dynamic pressure for parachute deploy or the atmosphere dust model, and the difference between the optimal and on-board atmospheric entry was negligible.

2. *Opportunity*

EDL Parameter Update #1 (After TCM-B4)

EDL parameter update #1 provided an opportunity to update the EDL sequence parameters following execution of TCM-B4. The analysis for this update was based on OD30 (delivered after TCM-B4 on January 18, 2004), a targeted parachute deploy dynamic pressure of 750 Pa, and atmosphere model "Ksv3.2.3 Special 5". The results of the analysis determined that an update was required, because both the targeted parachute deploy dynamic pressure and the atmosphere model had changed and the atmospheric entry time was 8 seconds earlier as a result of a larger than anticipated TCM-B4 maneuver, given that TCM-B3 had been canceled. The updated EDL parameters were uplinked to the spacecraft on January 18, 2004.

EDL Parameter Update #2 (After TCM-B5)

EDL parameter update #2 provided an opportunity to update the EDL sequence parameters following execution of TCM-B5. Even though TCM-B5 was not performed, an EDL parameter update analysis was carried out. This analysis was based on OD36 (delivered on January 23, 2004), a targeted parachute deploy dynamic pressure of 750 Pa, and atmosphere model "Ksv3.2.5 Special 7". The results of the analysis determined that no update was required. There was no change to the targeted dynamic pressure for parachute deploy, and, despite an update to the atmosphere, the difference between the optimal and on-board atmospheric entry time was negligible.

EDL Parameter Update #3 (With TCM-B6 Design)

EDL parameter update #3 provided an opportunity to update the EDL sequence parameters in the event that there was a late change in the trajectory (i.e., atmospheric entry conditions) whether or not TCM-B6 was executed. As has been noted previously, TCM-B6 was not performed. The EDL parameter update analysis was based on OD39 (delivered on January 23, 2004), a targeted parachute deploy dynamic pressure of 750 Pa, and atmosphere model "Ksv3.2.6 Special 9". The analysis determined that no update to the EDL parameters was required. There was no change to the targeted dynamic pressure for parachute deploy, and, despite an update to the atmosphere, the difference between the optimal and on-board atmospheric entry time was negligible.

VII. Real-time EDL Event Detection

The navigation team was responsible during EDL operations for attempting to detect and confirm the following EDL-related events (see Section IV.D), based on observations of DTE one-way X-band Doppler residuals:

E – 105 minutes	Transition from the cruise stage MGA to the cruise stage LGA (coincident with transition of the telecommunications system from two-way coherent mode to one-way mode)
E – 85 minutes	Turn to entry attitude
E – 40 minutes	HRS venting
E – 15 minutes	Cruise stage separation
E – 0 minutes	Atmospheric deceleration
~E + 4 minutes	Parachute deployment

Detection of these events was accomplished by observing real-time Doppler residuals as displayed by the Automated Radiometric Data Visualization and Real-time Correction (ARDVARC) program. Following the transition from two-way coherent mode to one-way mode, the process was considerably complicated by several factors: oscillator stability of the spacecraft radio transmitter, spacecraft acceleration, temperature changes caused by cycling of the HRS thermal valve, pressure effects, and Allan variance. It should be noted that, the indicator for detection of parachute deployment was, by definition, loss of lock on the one-way Doppler signal. Careful analyses by the EDL telecom analysts had demonstrated that, although it was likely that lock on the one-way Doppler signal would be preserved up to parachute deployment, spacecraft dynamics following parachute deployment guaranteed loss of lock on the one-way Doppler signal.

Despite the complicating factors noted in the preceding paragraph, the navigation team was successful in detecting each of the EDL events listed above for both *Spirit* and *Opportunity*. This was made possible not only by the distinct Doppler residual signature caused by each of these events, but also by virtue of extensive analyses and comprehensive procedural testing (using simulated one-way tracking data) carried out prior to EDL.

A detailed description of the process and results for real-time EDL event detection (including snapshots of ARDVARC displays for various events) is provided in [6].

VIII. Rover Position Determination

Following landing, the navigation team was responsible for determining the landing locations for the *Spirit* and *Opportunity* rovers in inertial coordinates based on the following types of radiometric tracking data: DTE X-band two-way Doppler from the rover and from the Mars Odyssey orbiter and UHF two-way Doppler between the rover and the Odyssey orbiter. The navigation team was also responsible for determining the position of the rovers after they had departed the landing sites, but only on an as-needed basis and given that the rovers remained essentially stationary for a sufficient time period. The rover position determination requirements are given in Section IV.E. The process used to determine the position of the rover on the surface and preliminary results are described in [9]. In addition to radiometric-based rover position determination by the navigation team, the science team used a process based on triangulation of visible landmarks to determine an independent estimate of the position of the rover.

A. *Spirit* Rover Position Determination

Figure 20-a shows the *Spirit* landing target, the final pre-entry estimated landing point ("Dispersion Center") and associated dispersion ellipses based on OD46, and the actual landing locations as estimated by the navigation team (using radiometric data) and the science team (using landmark triangulation).[8] Figure 20-b shows a blow-up of the region encompassing the final pre-entry estimates and the actual landing location. Note that the landing dispersions caused by navigation errors only (i.e., atmospheric entry delivery errors) are very small relative to the total size of the landing ellipse (unmargined or margined).

[8] In addition to the landing location solution shown in Fig. 20, a quick-look landing location estimate was generated about 2 hours after *Spirit's* landing based on DTE differenced one-way Doppler data through parachute deployment. The method and results for this quick-look estimate are discussed in [6].

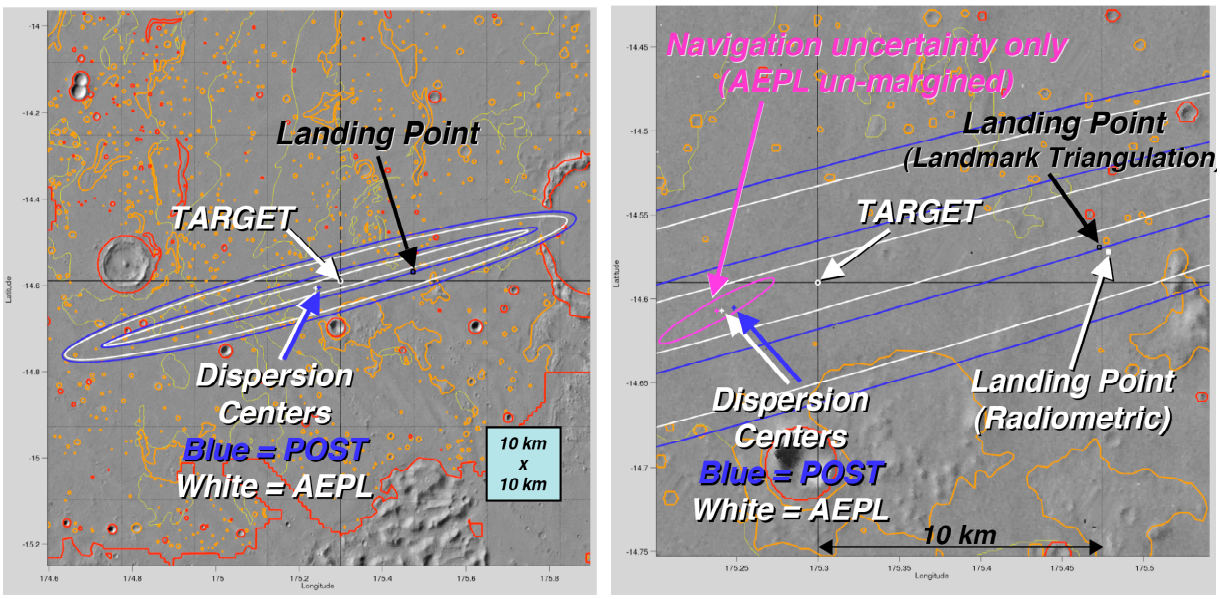

a) b)

Figure 20: *Spirit* final pre-entry landing estimate (OD46) and actual landing location.

The target landing point and the landing location as determined by the navigation team (with associated uncertainties) are given in Table 14. The navigation solution was based on two passes of two-way UHF-band Doppler between *Spirit* and the Odyssey orbiter plus several passes of two-way DTE Doppler. The navigation solution was delivered on January 9, 2004, about six days after landing. (It should be noted that only selected UHF passes in the first week or so following landing were configured as two-way coherent passes that were useful for landing location determination.) The 1-sigma uncertainties in latitude and longitude listed in Table 14 (converted to units of meters) are well within the 100 m (3σ) landing location accuracy requirement listed in Section IV.E.

Table 14: *Spirit* landing target and navigation estimate.

Parameter	Target (deg)	Navigation Solution			Error (deg)	Miss Distance (km)
		Value (deg)	Uncertainty (1σ) deg	Uncertainty (1σ) meters		
Latitude*	-14.59	-14.57189	1.14E-04	6.5	0.01811	10.1
Longitude*	175.30	175.47848	2.58E-06	0.2	0.17848	
*IAU/IAG 2000 coordinate system (areocentric).						

The final pre-entry estimated landing point from OD46 (based on radiometric data through E – 105 minutes) was 3.3 km uptrack from the target, whereas the actual landing point was determined to be 10.1 km from the target, mostly in the downtrack direction (see Fig. 20-b). The difference between final pre-entry estimated landing point and the actual landing point (13.4 km) is attributed to errors introduced by atmosphere and spacecraft aerodynamics modeling uncertainties. The difference between the landing locations as estimated by the navigation team (using radiometric data) and the science team (using landmark triangulation) was only 300 m. This difference was within the expected map-registration error.

A second rover position solution for *Spirit* was delivered on April 16, 2004 (about 104 days after landing). This solution was generated during a period of time when *Spirit* was stationary for purposes of uploading a new version of flight software. This solution indicated that *Spirit* was approximately 320 m from its landing position. For this solution, the 1-sigma uncertainties in latitude (4.0 m) and longitude (0.3 m) were well within the 30 m (3σ) rover position accuracy requirement listed in Section IV.E.

B. *Opportunity* Rover Position Determination

Figure 21-a shows the *Opportunity* landing target, the final pre-entry estimated landing point and associated dispersion ellipses based on OD41, and the actual landing locations as estimated by the navigation team (using radiometric data) and the science team (using landmark triangulation).[9] Figure 21-b shows a blow-up of the region encompassing the final pre-entry estimates and the actual landing location. Note that the landing dispersions caused

[9] In addition to the landing location solution shown in Fig. 21, a quick-look landing location estimate was generated about 10 minutes after *Opportunity's* landing based on DTE differenced one-way Doppler data through parachute deployment. The method and results for this quick-look estimate are discussed in [6].

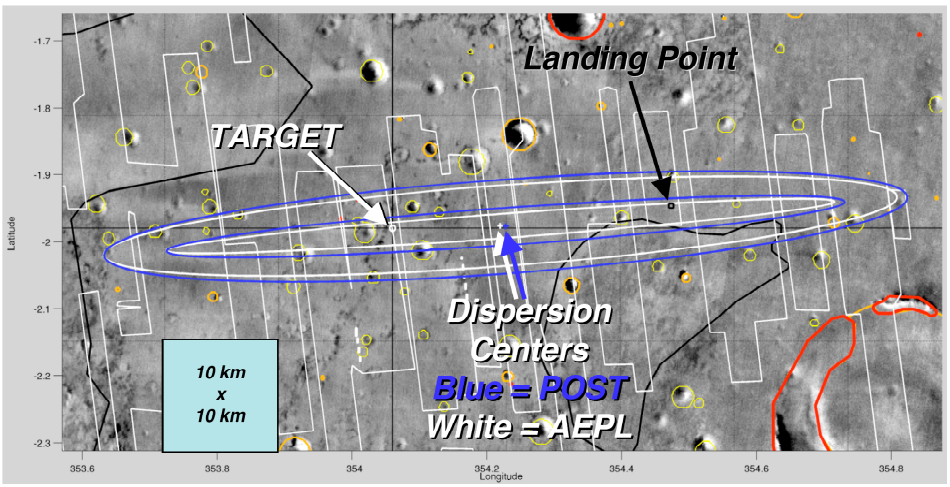

a)

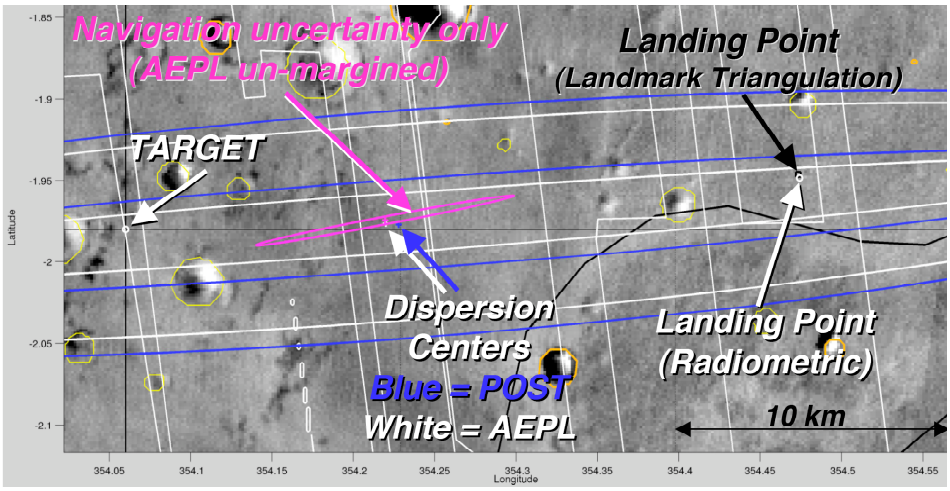

b)

Figure 21: ***Opportunity*** **final pre-entry landing estimate (OD41) and actual landing location.**

by navigation errors only (i.e., atmospheric entry delivery errors) is very small relative to the total size of the landing ellipse (unmargined or margined).

The target landing point and the landing location determined by the navigation team (with associated uncertainties) are given in Table 15. The navigation solution was based on two passes of two-way UHF-band Doppler between *Opportunity* and the Odyssey orbiter plus several passes of two-way DTE Doppler. The navigation solution was delivered on January 28, 2004, about four days after landing. (As for Spirit, only selected UHF passes in the first week or so following landing were configured as two-way coherent passes that were useful for landing location determination.) The 1-sigma uncertainties in latitude and longitude listed in Table 15 (converted to units of meters) are well within the 100 m (3σ) accuracy requirement listed in Section IV.E.

Table 15: ***Opportunity*** **landing target and navigation estimate.**

Parameter	Target (deg)	Navigation Solution			Error (deg)	Miss Distance (km)
		Value (deg)	Uncertainty (1σ) deg	Uncertainty (1σ) meters		
Latitude*	-1.98	-1.94828	1.23E-04	7.0	0.03172	24.6
Longitude*	354.06	354.47417	3.23E-06	0.2	0.41417	
*IAU/IAG 2000 coordinate system (areocentric).						

The final pre-entry estimated landing point from OD41 (based on radiometric data through E – 105 minutes) was 9.7 km downtrack from the target, whereas the actual landing point was 24.6 km downtrack from the target (see Fig. 21-b). The difference between final pre-entry estimated landing point and the actual landing point (14.9 km) is attributable to errors introduced by atmosphere and spacecraft aerodynamics modeling uncertainties. Note that the direction and magnitude of movement between the final pre-entry estimate and the actual landing location for

Opportunity are essentially the same as for *Spirit*. The difference between the landing locations as estimated by the navigation team (using radiometric data) and the science team (using landmark triangulation) was only 135 m (again within the expected map-registration error).

A second rover position solution for *Opportunity* was delivered on April 22, 2004 (about 89 days after landing). This solution was generated during a period of time when *Opportunity* was stationary for purposes of uploading a new version of flight software. This solution indicated that *Opportunity* was approximately 180 m from its landing position. For this solution, the 1-sigma uncertainties in latitude (9.3 m) and longitude (0.6 m) were within the 30 m (3σ) rover position accuracy requirement listed in Section IV.E.

IX. Conclusion

The system developed for navigating the two MER spacecraft to Mars was significantly improved relative to prior Mars missions. These improvements were necessary to achieve stringent atmospheric entry delivery requirements in order to yield landing dispersions that were small enough to ensure a high probability of a safe landing for both the *Spirit* and *Opportunity* landers. Prior to launch, the required atmospheric entry FPA delivery accuracies at TCM-5 (E – 2 days) were ±0.12° (3σ) for *Spirit* and ±0.14° (3σ) for *Opportunity*. Actual navigation performance far exceeded these requirements. The OD knowledge at the time TCM-5 was canceled was ±028° (3σ) for *Spirit* and ±0.035° (3σ) for *Opportunity*. The actual errors in entry FPA, based on the final pre-entry OD solutions, were estimated to be –0.007° for *Spirit* and +0.030° for *Opportunity*. (The entry FPA error for *Opportunity* would have been much smaller had TCM-B5 not been canceled to eliminate what was judged an unnecessary correction to the predicted landing location). These FPA errors correspond to errors in the magnitude of the B-vector of only 180 m for *Spirit* and 750 m for *Opportunity*. Navigation performance for *Spirit* was such that only four of six planned TCMs were required; TCMs A5 (E – 2 days) and A6 (E – 4 hours) were canceled. For *Opportunity*, only three of six planned TCMs were required; TCMs B3 (E – 65 days), B5 (E – 2 days) and B6 (E – 4 hours) were canceled.

Landing accuracy was also exemplary. The miss distances from the target landing point, caused solely by navigation errors at atmospheric entry, were only 3.3 km (uptrack) for *Spirit* and 9.7 km (downtrack) for *Opportunity*. Total miss distances, including errors introduced from atmosphere and spacecraft aerodynamics uncertainties, were 10.1 km (mostly downtrack) for *Spirit* and 24.6 km (downtrack) for *Opportunity*. These mostly along-track surface miss distances should be compared to the end-to-end lengths of the 99% probability target landing ellipses: 67 km (unmargined) or 78 km (margined) for *Spirit* and 74 km (unmargined) or 85 km (margined) for *Opportunity*.

During EDL operations, the navigation team was able to successfully detect and confirm the following events for both *Spirit* and *Opportunity* based on real-time displays of DTE one-way X-band Doppler residuals: transition from cruise stage MGA to cruise stage LGA, turn to entry attitude, HRS venting, cruise stage separation, atmospheric deceleration, and parachute deployment.

After the *Spirit* and *Opportunity* landings, actual landing locations were determined based on DTE X-band two-way Doppler and UHF two-way Doppler between the rovers and the Odyssey orbiter. The uncertainties of these landing location estimates were on the order of about 20 m (3σ) for latitude and less than 1 m (3σ) for longitude. These uncertainties were well within the required 100 m (3σ) accuracy.

As with every flight project, there were numerous lessons learned from the MER development and flight operations phases. These lessons learned included many that are applicable to interplanetary navigation. The lessons learned in the area of interplanetary navigation based on the MER experience are listed in Appendix A.

References

[1] Portock, B. M., Graat, E. J., McElrath, T. M., Watkins, M. M., and Wawrzyniak, G. G., "Mars Exploration Rovers Cruise Orbit Determination," *AIAA/AAS Astrodynamics Specialist Conference*, AIAA-2004-4981, AIAA, Washington, DC, 2004.

[2] McElrath, T. P., Watkins, M. M., Portock, B. M., Graat, E. J., Baird, D. T., Wawrzyniak, G. G., Guinn, J. R., Antreasian, P. G., Attiyah, A. A., Baalke, R. C., and Taber, W. L., "Mars Exploration Rovers Orbit Determination Filter Strategy," *AIAA/AAS Astrodynamics Specialist Conference*, AIAA-2004-4982, AIAA, Washington, DC, 2004.

[3] Wawrzyniak, G. G., Baird, D. T., Graat, E. J., McElrath, T. P., Portock, B. M., and Watkins, M. M., "Mars Exploration Rovers Orbit Determination System Modeling," *AIAA/AAS Astrodynamics Specialist Conference*, Providence, AIAA-2004-4983, AIAA, Washington, DC, 2004.

[4] Kangas, J. A., Potts, C. L., and Raofi, B., "Mars Exploration Rovers Launch Performance and TCM-1 Maneuver Design," *AIAA/AAS Astrodynamics Specialist Conference*, AIAA-2004-4984, AIAA, Washington, DC, 2004.

[5] Potts, C. L., Raofi, B., and Kangas, J. A., "Mars Exploration Rovers Propulsive Maneuver Design," *AIAA/AAS Astrodynamics Specialist Conference*, AIAA-2004-4985, AIAA, Washington, DC, 2004.

[6] Baird, D. T., McElrath, T. P., Portock, B. M., Graat, E. J., Wawrzyniak, G. G., Knocke, P. C., D'Amario, L. A., Watkins, M. M., Craig, L. E., and Guinn, J. R., "Mars Exploration Rovers Entry, Descent, and Landing Navigation," *AIAA/AAS Astrodynamics Specialist Conference*, AIAA-2004-5091, AIAA, Washington, DC, 2004.

[7] Desai, P. N., and Knocke, P. C., "Mars Exploration Rovers Entry, Descent, and Landing Trajectory Analysis," *AIAA/AAS Astrodynamics Specialist Conference*, AIAA-2004-5092, AIAA, Washington, DC, 2004.

[8] Knocke, P. C., Wawrzyniak, G. G., Kennedy, B. M., Parker, T. J., Golombek, M. P., Duxbury, T. C., Kass, D. M., and Desai, P. N., "Mars Exploration Rovers Landing Dispersion Analysis," *AIAA/AAS Astrodynamics Specialist Conference*, AIAA-2004-5093, AIAA, Washington, DC, 2004.

[8] Seidelmann, P. K., Abalakin, V. K., Bursa, M., Davies, M. E., De Bergh, C., Lieske, J. H., Oberst, J., Simon, J. L., Standish, M. E., Stooke, P, and Thomas, P. C., "Report of the IAU/IAG Working Group on Cartographic Coordinates and Rotational Elements of the Planets and Satellites: 2000," *Celestial Mechanics and Dynamical Astronomy*, Vol. 82, 2002, pp. 83-110.

[9] Guinn, J. R., and Ely. T. A., "Preliminary Results of Mars Exploration Rover In-Situ Radio Navigation," *AAS/AIAA Space Flight Mechanics Meeting*, AAS-04-270, AAS, Springfield, VA, 2004.

Appendix A
MER Navigation Lessons Learned

The lessons learned from MER in the area of interplanetary navigation were derived from inputs provided by the members of the MER navigation team. These lessons learned are as follows:

- Navigation and entry, descent, and landing (EDL) must be viewed together as a complete end-to-end system, involving all aspects of OD, maneuver, flight system capabilities, site selection, EDL capabilities, timelines, etc. Separating the components and then relying purely on interfaces does not work. Overlapping, system-oriented, communicative teams are needed in these areas.

- Exceptional performance (and cost value) can be generated by project teams working closely with their line organizations to fully understand capabilities and margin, how to push the performance envelope within reasonable risk and cost constraints, and how to further reduce risk through application of best practices and ongoing review.

- ΔDOR measurements significantly improved navigation delivery accuracy and provided complementary data to diagnose anomalous tracking data, unpredicted spacecraft dynamics, and anomalous interplanetary media effects.

- Performing ACS/NAV characterizations proved extremely useful both for verifying ACS performance and for reducing assumed ACS residual ΔV values, which translated into improved delivery accuracy.

- Development of a new OD scripting architecture allowed processing and evaluation of a large number of cases using different filter assumptions, which provided a high level of confidence in the OD solutions.

- Successful execution of extremely short templates (several hours) for late approach maneuver development would not have been possible without updating the process based on deficiencies uncovered during operation readiness tests (ORTs).

- Atmospheric entry targeting requires detailed analysis and special targeting strategies due to trajectory control correlations. This analysis and strategy should be coordinated across project elements, including navigation, EDL, and the flight system.

- Atmospheric entry targeting requirements placed on navigation need further clarification. The requirements should state the desired mean entry flight path angle (FPA) with some "not to exceed" bounds based upon the flight system capability, along with the 3-sigma FPA delivery accuracy. (The objective is to avoid the misconception that the FPA had to be the nominal value of -11.5° for MER.)

- Visualization of landing dispersions and associated statistical calculations (e.g., probability of in-spec landing) were indispensable to landing site selection and the decision process for final approach trajectory correction maneuvers (TCMs).

- Processing differenced one-way X-band Doppler collected during EDL provided, within a few hours of landing, a quick estimate of the landing location accurate to within a few kilometers (independent of landing success).

- Two passes of in-situ (lander-orbiter) two-way UHF Doppler data plus a small amount of DTE two-way X-band Doppler data (from the lander/rover) permit determination of the lander/rover position in inertial space accurate to within a few 10s of meters.

- Staffing the Emergency Control Center, located at the Lockheed Martin Astronautics facility in Denver, for backup navigation support (and the infrastructure preparations that were required to do this) was extremely successful.

Appendix B
Abbreviations and Acronyms

ACS	attitude control system
APXS	Alpha-Particle X-Ray Spectrometer
ARDVARC	Automated Radiometric Data Visualization and Real-time Correction (program)
CCAFS	Cape Canaveral Air Force Station
CLS	central landing site
ΔDOR	delta-differenced one-way ranging
ΔV	velocity change
DESCANSO	Deep Space Communications and Navigation Systems Center of Excellence
DLA	declination of the launch asymptote
DOF	degree of freedom
DSN	Deep Space Network
DTE	direct-to-Earth
EDL	entry, descent, and landing
EOP	Earth orientation parameters
ESF	Entry State File
ETLF	Entry Target and Landing File
FPA	flight path angle
HEF	high-efficiency (antenna subnet)
HGA	high gain antenna
HRS	heat rejection system
IAG	International Association of Geodesy
IAU	International Astronomical Union
IDD	Instrument Deployment Device
IMU	inertial measurement unit
LGA	low-gain antenna

MER	Mars Exploration Rover
MER-A	Spirit Mars Exploration Rover
MER-B	Opportunity Mars Exploration Rover
M-FSK	multiple-frequency shift key
MGA	medium-gain antenna
MGS	Mars Global Surveyor
Mini-TES	Miniature Thermal Emission Spectrometer
MOC	Mars Orbiter camera
nrad	nanoradian
ns	nanosecond
OD	orbit determination
ODY	Mars Odyssey
ORT	Operations Readiness Test
Pancam	Stereo Panoramic Imager
PDPF	Parachute Deploy Parameter File
RAD	rocket assisted deceleration
RAT	Rock Abrasion Tool
RMDC	Radiometric Data Conditioning (group)
SDST	small deep-space transponder
SMAA	semi-major axis
SMIA	semi-minor axis
SSPA	solid-state power amplifier
TCA	time of closest approach
TCM	trajectory correction maneuver
UHF	ultra high frequency